

# CASE FILE COPY

N69-38272  
TMX-53898

## NASA TECHNICAL MEMORANDUM

Report No. 53898

### A NEW INTERPRETATION OF THE EXPLORER XVII AND EXPLORER XXXII IONIZATION GAUGE DATA AND ITS IMPLICATIONS TO ORBITAL ANALYSIS

By James O. Ballance  
Aero-Astroynamics Laboratory

September 11, 1969

**NASA**

*George C. Marshall Space Flight Center  
Marshall Space Flight Center, Alabama*

1. REPORT NO. TM X-53898	2. GOVERNMENT ACCESSION NO.	3. RECIPIENT'S CATALOG NO.	
4. TITLE AND SUBTITLE A NEW INTERPRETATION OF THE EXPLORER XVII AND EXPLORER XXXII IONIZATION GAUGE DATA AND ITS IMPLICATIONS TO ORBITAL ANALYSIS		5. REPORT DATE September 11, 1969	
		6. PERFORMING ORGANIZATION CODE	
7. AUTHOR(S) James O. Ballance		8. PERFORMING ORGANIZATION REPORT #	
9. PERFORMING ORGANIZATION NAME AND ADDRESS NASA - George C. Marshall Space Flight Center Marshall Space Flight Center, Alabama 35812		10. WORK UNIT NO.	
		11. CONTRACT OR GRANT NO.	
12. SPONSORING AGENCY NAME AND ADDRESS		13. TYPE OF REPORT & PERIOD COVERED  Technical Memorandum	
		14. SPONSORING AGENCY CODE	
15. SUPPLEMENTARY NOTES			
16. ABSTRACT  <p>The response of the modified Redhead magnetron density gauges used on the Explorer XVII and Explorer XXXII satellites has been analyzed by using the transmission probabilities and time response characteristics due to geometry and gas-molecule/surface interactions. It was found that the very evident fluid dynamic response characteristics of the data required an interpretation which uses low energy and momentum exchange for the gas on the initial wall collisions with total loss of atomic oxygen. An additional signal due to a process -- most likely to be recombination -- taking place on the wall of the gauge is suggested. For the example used, there is a factor of two between the derived density based on the original assumptions and the density based on the new interpretation.</p>			
17. KEY WORDS		18. DISTRIBUTION STATEMENT PUBLIC RELEASE:  <i>E. D. Geissler</i> E. D. Geissler Director, Aero-Astroynamics Laboratory	
19. SECURITY CLASSIF. (of this report)  UNCLASSIFIED	20. SECURITY CLASSIF. (of this page)  UNCLASSIFIED	21. NO. OF PAGES  43	22. PRICE

A NEW INTERPRETATION OF THE EXPLORER XVII  
AND EXPLORER XXXII IONIZATION GAUGE DATA AND  
ITS IMPLICATIONS TO ORBITAL ANALYSIS

SUMMARY

The response of the modified Redhead magnetron density gauges used on the Explorer XVII and Explorer XXXII satellites has been analyzed by using the transmission probabilities and time response characteristics due to geometry and gas-molecule/surface interactions. It was found that the very evident fluid dynamic response characteristics of the data required an interpretation which uses low energy and momentum exchange for the gas on the initial wall collisions with total loss of atomic oxygen. An additional signal due to a process -- most likely to be recombination -- taking place on the wall of the gauge is suggested. For the example used, there is a factor of two between the derived density based on the original assumptions and the density based on the new interpretation.

I. INTRODUCTION

There has been a consistent difference between the values for the density of the upper atmosphere as derived from ionization type gauges (pressure gauges, mass spectrometers, etc.) flown on sounding rockets and satellites and the density derived from satellite drag [1,2,3,4,5, 6]. Those groups which conduct experimental probe studies of the upper atmosphere suggest that the cause for this difference is in the coefficients used in the drag analysis; whereas, the groups which conduct the drag analysis suggest that the cause is in the interpretation of gauge data. Each group has valid arguments, and since there has not been any truly definitive experiments conducted to determine the cause, either position can be defended without much difficulty.

Perhaps the best available series of experiments conducted which could help define the cause of the problem are the aeronomy satellites of the Goddard Space Flight Center [1,2,7,8,9,10,11]. Explorer XVII (AE-A) and Explorer XXXII (AE-B) had a basic structure ideal for the drag analysis (a sphere  $\approx$  88 cm in diameter), as well as several types of ionization gauges used to measure density. It was from the Explorer XVII data that a consistent factor of two between the gauge-measured

density and drag-derived densities occurred. Numerous reasons have been examined in an attempt to explain the differences; none seem to fully describe the problem. At the risk of merely adding more confusion, this paper offers a new interpretation of the ionization gauge data and its implication both to the use of ionization gauges and to orbital analysis of satellites for determining upper atmosphere densities.

In addition to the advantage of the geometry of the aeronomy satellites, both AE-A and AE-B had, among their complement of instruments, identical cold cathode magnetron ionization gauges to measure the density. Furthermore, from a Monte Carlo analysis of the two types of density gauges on AE-A [2], the magnetron gauge (due to its internal geometry) was seen to be the more sensitive to various models of gas-surface interactions used in the study. Also, the spin rate of AE-B was about one-third that of AE-A. Thus, the same gauge could be analyzed both in terms of the gas-surface interaction model and its time response.

The details of that analysis are presented in this report. First, the measured data are examined and adjusted for obvious characteristics of the system. Next, the theoretical response of the gauge is presented for several gas-surface interaction models and their time response characteristics, and compared with the measured data. From this comparison, the physical processes taking place are suggested. Based on this indication, a simple model which yields amazingly similar results with respect to the measured data is developed. Using this model, we examine the general characteristics of drag coefficients to see what change would be expected, if any, in the orbital drag analysis.

## II. FLIGHT DATA

### A. Ionization Gauge Operation

The modified Redhead is a member of the large family of ionization pressure gauges. As the term implies, the neutral molecules which are introduced into the sensing volume are ionized, and the resulting ions are collected and counted. When there are steady state conditions, an ion current is measured which is related to the pressure in the following way:

$$I = k P^N,$$

where

I = ion current

k = sensitivity factor

P = pressure

N = constant usually lying between 1.1 and 1.4.

In a mixture of gases, the sensitivity for each of the constituents must be known to interpret the measurements. In any case, however, the measured current is proportional to the number density of the gas mixture in the sensing volume.

### B. Flight Data

Figure 1 presents a typical data sheet, graciously provided by Mr. George Newton, GSFC, showing the time and the equivalent  $N_2$  pressure for the current measured. The left group of columns gives this information for the time indicated, while the right group of columns gives the data for  $t + .025$  seconds.

The data were adjusted in the following manner. First, since the measured densities must be proportional both to any outgassing in the gauge and to the ambient density which is dependent on the relative motion between the gauge and the atmosphere, a complete spin cycle was examined to find the minimum pressure before the next maximum value. This pressure was then subtracted from a complete tumble cycle starting with that point, leaving a table of data which depended only on the processes above, principally, the fluid dynamics due to the motion. These data were then normalized to the maximum pressure in the table and the results plotted (see figure 2). In all cases, a very obvious discontinuity occurred (such as seen at about 75 and 150 degrees in figure 2) at about the same pressure level, due to a calibration constant change in the data reduction program. The data were then shifted as indicated in figure 2 and renormalized. The final data plots are shown in figure 3. Thus, the number density history of a complete spin cycle was achieved.

Inspection of the data reveals several interesting characteristics. First, if one considers the response to be equivalent to that of an orifice system with the peak pressure indicating the value at the minimum angle of attack, then the ratio of the pressure at  $\alpha_{\min}$  to that at  $\alpha_{90^\circ}$  should indicate the speed ratio. From figure 3, we see that this ratio is approximately 20.2, indicating  $S = 5.7$ . Since  $S = U \cos(\alpha)/V_m$ , it follows that

$$V_m = [2kT/m]^{1/2} = U \cos(\alpha)/S$$

$$\approx 1400 \text{ m/sec.}$$

If the gas were  $N_2$ , then the exospheric temperature would be about 3400°K, which is an unacceptable result. A further look at the data easily discounts this consideration. If the measured data were purely a fluid dynamic response of an orifice in a hypersonic free molecule flow, there should be symmetry about the peak pressure. Very evidently this is not the case in the measured data. The next approach then would be to examine the data as a pressure probe response. This will be done in Section III.

### III. THEORETICAL PREDICTIONS

#### A. Probe Response

The response of a probe moving in a gas in free molecular flow and under equilibrium conditions is given by

$$P_s = P_o (T_o/T_s)^{1/2} F(S) \frac{K_o(G, S, \alpha)}{K_o(G, 0, 0)},$$

where

$P_s$  = pressure in the sensor

$P_o$  = pressure of the ambient gas

$T_s$  = temperature of the sensor

$T_o$  = temperature of the ambient gas

$F(S) = e^{-S^2} + \pi^{1/2} S [1 + \text{ERF}(S)]$

$S = U \cos(\alpha)/V_m$

$U$  = mass velocity of the probe relative to the gas

$\alpha$  = angle between the normal to the orifice and the velocity vector

$V_m$  = most probable speed of the molecules

$K_O(G,S,\alpha)$  = transmission probability in free molecular flow for the geometry connecting the ambient flow to the sensor volume.

The factor  $K_O(G,S,\alpha)$  is a function of the geometry (G), the relative speed (S), the angle of attack ( $\alpha$ ), and the gas-surface interaction model. For free molecule flow with no mass flow, the molecules striking a surface are reflected diffusely. An analysis of sounding rocket probe data when the speed ratio was small (i.e.,  $\approx 2-3$ ) indicated that the reflections were diffuse; however, there was little difference between the response considering a model using completely diffuse reflections and a model when every molecule was specularly reflected on its first collision [13].

The Monte Carlo analysis of the geometry of the modified Redhead gauge shows a significant change in the response of the system at high speed ratios with various gas-surface interaction models (see figure 4). A simple program was written to calculate the theoretical response of the Redhead gauge as a function of the spin angle of the satellites. The transmission probabilities calculated by the Monte Carlo method were fitted by a least-squares curve-fitting routine, and the responses for the three gas-surface interaction models were determined. As in the flight data, the results were normalized to the maximum value that occurred at the minimum angle of attack. Figures 5, 6, and 7 present typical results.

In all cases these model results exhibit complete symmetry about the minimum angle of attack. This feature is due to the assumption of equilibrium conditions at every instant of time in the spin cycle. In general, the increase in the number of specular reflections results in a much broader response characteristics. The dip in the specular reflection near the peak response is due to the assumption of completely specular reflection even when the angle of incidence of the molecules onto the top electrode of the gauge is almost normal. At the high energies of gas molecule/satellite-surface interactions, this assumption does not seem valid; therefore, the transmission probabilities for the one specular case were adjusted to more nearly fit the diffuse reflection case for 0 and 5 degrees angle of attack, resulting in the final set of data shown in figure 8. Actually, this adjustment has little effect on either the shape of the curve or the absolute value of the number densities.

## B. Probe Response with Time Response

In the Monte Carlo calculation of the transmission probabilities, other information about the response of the gauge was also obtained. One feature was the time history of the molecules entering the gauge until they reached the sensing volume. Figure 9 presents typical results showing the time required for the total number of molecules to reach the sensing volume for three angles of attack. Actually, the values for 30 degrees angle of attack are essentially identical to those for all angles of attack from 30 to 90 degrees. Although 70 to 80 percent of the molecules can be sensed in about 10 milliseconds, the total number has not arrived at the sensor until about 150 milliseconds.

Satellites AE-A and AE-B had spin rates of 0.67 sec/rev and 2.0 sec/rev, respectively. In terms of milliseconds per degree of spin, these rates are  $\approx 1.0$  and  $\approx 5.6$ . Thus, when 70 percent of the molecules reached the sensing volume in AE-A, the angle of attack had changed by 5 degrees, and in AE-B by 2 degrees. The idea of complete equilibrium at each instant of time for the probe analysis was obviously wrong. Accordingly, the analysis was modified to provide for this feature in the following manner. Using the transmission probabilities, the number of molecules entering the orifice which will reach the sensor in a small increment of spin angle was calculated. The time for that number to arrive at the sensor was then determined from the time response characteristics derived from figure 9. Within the sensor, however, molecules were leaving at any instant of time, some of which would return to the ambient field and some to the sensor. The flow from the sensor volume to ambient conditions was calculated for the geometry of the gauge with Monte Carlo techniques, along with the time history for returning molecules. With all of this information, the number density within the sensor volume was calculated as a function of the spin rate. Mathematically, this would be expressed as

$$(N_{\text{total}})_j = N_j K_j \Delta t_j + \sum_{i=1}^{j-1} [N_i K_i \Delta t_i - (N_{\text{total}})_i K_R \Delta t_R],$$

where

$(N_{\text{total}})_j$  = number density in the sensing volume at a spin angle  $j$ .

$N_j$  = average number of molecules entering the orifice during the change in spin angle for  $j-1$  to  $j$ .

$K_j$  = probabilities that the molecule will not return to its present position.



$\Delta t_j$  = fraction of molecules which will exit or be counted in the time corresponding to the change of spin angle for  $j-1$  to  $j$ .

Typical results of these calculations are shown in figures 10, 11, and 12. While the general shape of the curve is unchanged by the time integration, the symmetry about the minimum angle of attack which occurs under equilibrium conditions is gone. Even more evident, however, is the change in the magnitude. Figure 13 presents a typical theoretical pressure response for the equilibrium probe response and the time-integrated response.

#### C. Probe Response with Time Response Plus Gas Evolution

Although the time integration procedure closely predicts the measured values, it is still very evident that some other additional process is affecting the data. The effect is certainly not symmetrical since the deviation is greater as the measured signal has passed its peak value and begins to fall. This fact suggests that, whatever the process or processes taking place, they are proportional to the total number of molecules which had entered the probe. To test this hypothesis, the previous integration procedure was modified to include an additional term proportional to the total number density which has entered the probe before each counting period. The proportionality factor must obviously be a function of the gas species, the ratios of gas species, the geometry of the probe, the angle of attack, the sticking probability, the recombination probability, etc. Since none of these relations are known, the factor was assumed to be constant and various values were tried. The results are shown in figure 14 for factors of 0.01, 0.001, and 0.0001. The predicted response with the factor of .001 is only partially shown. Since the best fit to the data seems to be that model, the comparison is repeated for that case in figure 15, where a very good correlation occurs.

#### D. Spin Rate Effects

The flight measurements are for the Explorer XXXII, when its spin rate was 0.5 cycle/second. All of the previous analysis considered this same rate; however, since the Explorer XVII rate was 1.5 cycles/second, the analysis was repeated for this faster rate. Figure 16 presents the case of one specular reflection and the factor of .001. While, in general, the theoretical analysis does approach closely the flight measurements for the lower spin rate, the agreement is not nearly so good when the correct rate is used.

### E. Magnitude of Response

Although the normalized graphical display of the response characteristics are extremely useful in developing the concepts for the physical process occurring in the gauge, the magnitude of the response curve is required to relate the measured density to the ambient density. Figure 17 shows the predicted magnitude response for (1) an orifice analysis, (2) an equilibrium pressure probe analysis, (3) a time-integrated probe response with one specular reflection and the factor of .001 with a 0.5 cycle/second spin rate, and (4) the time-integrated probe response with a 1.5 cycle/second spin rate. It is easily noticeable that the integrated response values for both spin rates are within  $\pm 10$  percent of the orifice response value at  $\alpha_{\min}$ .

Figure 18 compares the integrated response values with and without the additional factor. Again, at the peak value, the increase in the number density is only about 10 percent. Figure 19 shows the integrated response with the additional factor for two surface-interaction models. While the shapes of the curves differ, it is seen that the magnitudes of the number density at  $\alpha_{\min}$  are identical.

## IV. DISCUSSION OF RESULTS

### A. Angle of Attack Effects

Although the above analysis has been discussed only for the case when  $\alpha_{\min} = 0$  degrees, data were also available for  $\alpha_{\min} = 10$  degrees and  $\alpha_{\min} = 30$  degrees. Figures 20 and 21 present the flight data for  $\alpha_{\min} = 10$  degrees and the integrated time response for both the diffuse and one specular-reflection model including the additional factor. These curves appear to display essentially the same features as the  $\alpha_{\min} = 0$  degrees results. Similar results for the  $\alpha_{\min} = 30$  degrees analysis are shown in figures 22 and 23, where we can see that, while there is really little difference between the two models, the completely diffuse model actually seems to be more similar to the flight data.

These features imply that a more realistic model would be one in which the type of reflection is a function of the angle of incidence made by the gas molecule trajectory with the gauge surfaces. When the trajectory makes a small angle with respect to the normal to the surface at the point of collision, the reflection is more likely to be diffuse than when the angle is large (for example, when the molecule has a grazing collision where the trajectory is nearly parallel to the surface).

## B. Composition of the Atmosphere

In the previous analysis, the species of gas entering the probe has not been considered. The flight data used for this study represent measurements in altitude greater than 280 kilometers. At these altitudes the principal constituent of the atmosphere is atomic oxygen, the properties of which are essentially unknown, especially in terms of the energy and momentum exchange occurring at the very high relative velocity impact between the spacecraft and the molecule. Although some definitive measurements have been attempted, many questions still exist [14].

Because atomic oxygen is a very reactive particle, the probability that an oxygen atom, upon entering the probe and colliding with the wall several times, will become chemisorbed or physically adsorbed must be quite high. From the Monte Carlo analysis of the geometry of the pressure probe, it can be seen in figure 24 that, while a small percentage ( $\approx 25$  percent) of the molecules at small angles of attack may enter the sensor volume with less than 4 or 5 collisions with the walls, most of the particles must undergo many collisions before entering the sensor region. In fact, the particles were tracked for at least 350 collisions before they were discarded. (Fewer than 1 percent of the particles made more than 350 collisions before they entered the sensor region or returned to the ambient flow).

It seems reasonable to assume that atomic oxygen does not respond in the way the "billiard ball" model of the Monte Carlo method predicts. Most likely, the atomic oxygen "thermalizes" (i.e., assumes a velocity distribution described by the temperature of the probe) within a very few collisions (2 to 6), after which time it becomes bound to the wall by some chemical or physical process. Thus, the ion gauge on the satellite does not measure any appreciable amount of atomic oxygen.

However, from the analysis above it is quite evident that the responses of the density gauge on AE-A and AE-B were very similar as predicted from fluid dynamic considerations. There must be some constituent which must not have been captured onto the walls. Since the next major constituent of the atmosphere at these altitudes is molecular nitrogen, the response must be due to this gas.

In summary, the orbiting gauges respond to molecular nitrogen as predicted by fluid dynamic considerations, but little or no atomic oxygen is measured by these gauges.

### C. Processes within the Gauges

In this analysis it is evident that adequate correlation between the flight data and predicted data requires an additional process which is proportional to the integrated number of molecules having entered the probe before the time of measurement. Since the principal response is due to fluid dynamic characteristics of molecular nitrogen, what is the physical interpretation of the additional process? In terms of absolute magnitudes, species, etc., it is not possible to quote valid results because of the many unknowns listed above. Some insight, however, on the problem can be gained from the discussion of the previous section. Atomic oxygen must play the dominant role in this response. The additional signal is most likely due to molecular oxygen formed from the interaction of the oxygen atoms on the chamber walls or from the interaction of an incoming oxygen atom striking another one on the wall. Possibly the energy released by a high velocity atom frees loosely bound atoms on the wall which eventually recombine to form oxygen molecules. Another possibility which has been suggested by von Zahn is the formation of  $N_2O$  [15].

### D. Density Calculations

The interpretation used above reflects a great change in the densities derived from the gauge when compared to previous analysis. Newton's method for deriving density uses the expression:

$$\rho = \frac{(P_{\max} - P_{\min})}{V_{mp} U_n \pi^{1/2}}$$

where

$P_{\max}$  = maximum pressure in a tumble cycle

$P_{\min}$  = minimum pressure in a tumble cycle

$V_{mp}$  = the most probable speed of the gas in the sensor

$U_n$  = the relative normal velocity between the atmosphere and the probe.

Using the data from turn on #68 and assuming the ambient temperature to be  $10^3$  °K and the sensor temperature to be 300°K, the density was determined to be

$$\rho \approx 1.09 \times 10^{-14} \text{ gm/cm}^3$$

with the ratio of  $[O]/[N_2] = 3$ , so that  $\bar{m} = 19$ ;  $P_{\max} = 6.12 \times 10^{-7}$  mm Hg  $= 8.16 \times 10^{-3}$  dynes/cm<sup>2</sup>;  $P_{\min} = 2.8 \times 10^{-8}$  mm Hg  $= 3.73 \times 10^{-4}$  dynes/cm<sup>2</sup>;  $V_{mp} = 512$  m/sec,  $U_n = 8300$  m/sec. However, this value for density is valid only if the sensitivity of the gauge for atomic oxygen is the same as it is for molecular nitrogen. Most likely, the sensitivity factor for atomic oxygen is about 0.5 that for molecular nitrogen. For the  $[O]/[N_2]$  ratio above, the contributions of the two constituents to the total indicated pressure in the gauge is in the ratio of 1/1.5. Adjusting the response for this feature, the "true"  $P_{\max}$  would be  $1.32 \times 10^{-2}$  dynes/cm<sup>2</sup> and

$$\rho = 1.76 \times 10^{-14} \text{ gm/cm}^3.$$

Using the results of this study, we find that the speed ratio is about 10. Considering equal response of the gauge to  $N_2$  and the "recombination product,"  $N_2$  makes up about 93 percent of the maximum signal. The  $N_2$  density based on a pressure probe is

$$\rho = \frac{m}{kt} P[T_o/T_s] \gamma$$

where

$m$  = mass of an  $N_2$  molecule

$k$  = Boltzman's constant

$T$  = 1000°K

$P_{\max} = [8.16 \times 10^{-3} \text{ dyne/cm}^2] \times .93$

$\gamma$  = response factor determined by the analysis above = 35.4.

Evaluating this, we find

$$\rho_{n_2} = 1.24 \times 10^{-14} \text{ gm/cm}^3$$

since  $[O]/[N_2] = 3$ ,

$$\begin{aligned} \rho_{\text{total}} &= \rho_{n_2} + \rho_o \\ &= [1.24 \times 10^{-14} + 2.12 \times 10^{-14}] \text{ gm/cm}^3 \\ &= 3.36 \times 10^{-14} \text{ gm/cm}^3. \end{aligned}$$

Thus, it is seen that the density based on this study is about two times greater than that deduced by Newton's method.

#### E. Implications to Orbital Aerodynamic Calculations

If the results discussed above truly represent the gas-surface interactions at orbital conditions, it is interesting to see how these effects influence the more conventional aerodynamic calculations. Let us assume that the atmosphere is principally atomic oxygen and molecular nitrogen in the ratio  $[O]/[N_2]$  of 1 at 200 km and 8 at 300 km. Since the molecular nitrogen is specularly reflected, it seems reasonable that the energy exchange on colliding with the satellite surface is incomplete and the accommodation coefficient will be low. For convenience, we let the accommodation coefficient

$$ACC = \frac{E_i - E_r}{E_i - E_w}$$

be 0.5 for nitrogen.

Thus, for a spherical satellite, the drag coefficient at both 200 and 300 kilometers will be approximately 2. However, a satellite consisting of many flat surfaces will be affected as shown in figure 24, where the drag of a flat plate is shown for the assumed conditions.

#### V. CONCLUSIONS

From this analysis of the characteristics of the modified Redhead magnetron vacuum gauge flown on Aeronomy Satellites A (Explorer XVII) and B (Explorer XXXII), the following conclusions may be drawn:

a. The response of the gauge is not as predicted by equilibrium orifice theory or pressure probe theory because of the time response characteristics of the gauge and the spin rate of the satellites.

b. The response is basically a fluid dynamic, time-integrated signal which can be predicted by a simple, yet plausible, gas-surface interaction model.

c. The physical properties of the atmospheric gases being measured and the kinetics of the gases within the probe indicate that molecular nitrogen is the principal constituent being measured with some small contribution from processes such as recombination of atomic oxygen into molecular oxygen.

d. The gas-surface interaction model used for this analysis implies that aerodynamic coefficients must differ from those now calculated using diffuse reflection theories.

e. A critical need in the space physics area is a series of definitive experiments to establish the true interactions of the upper atmosphere with space probes.

## VI. RECOMMENDATIONS

Clearly, an experiment or a series of experiments needs to be conducted to answer these rather fundamental questions which plague both the space scientist and the space engineer. The Odyssey program of the Marshall Space Flight Center outlines several useful experiments which should be accomplished. These experiments are basically aerodynamically oriented from the viewpoint of orbital characteristics. To examine the gauge problem more closely, new experiments exploiting features observed in this type of analysis should be developed. Specifically, the idea of Zukov et al. [16] to use an orifice probe and a pitot probe to directly measure the upper atmospheric temperature could be expanded to include several pitot probes of the same design but with minor geometric changes which could allow examination of other parameters. That experiment would be extended to include cylindrical ducts of several length-to-radius ratios. In any case, the experiments should allow for:

a. Analysis of the free molecule flow properties of the probe by simple numerical methods. Various interaction models could thus be easily studied.

b. Spin modulation through all angles of attack but with spin rates sufficiently low to remove problems due to time response characteristics.

c. A mass spectrometer sensing element so that individual constituents could be analyzed.

d. A complete measurement through perigee to apogee and back to perigee.

e. Various types of gauge wall materials, such as stainless steel glass, etc.

GCA=	1	68	69	843	CURR1	PRESS1	ADV2	CURR2	PRESS2
TIME	ADV1								
34003.583	3.366	0.178E-05	0.473E-06	3.341	0.180E-05	0.481E-06			
34003.633	3.329	0.182E-05	0.485E-06	3.366	0.178E-05	0.473E-06			
34003.683	3.417	0.172E-05	0.458E-06	3.479	0.165E-05	0.438E-06			
34003.733	3.566	0.156E-05	0.412E-06	3.654	0.146E-05	0.385E-06			
34003.783	3.741	0.137E-05	0.359E-06	3.816	0.129E-05	0.336E-06			
34003.833	3.878	0.122E-05	0.317E-06	3.954	0.114E-05	0.295E-06			
34003.882	4.029	0.103E-05	0.272E-06	4.091	0.988E-06	0.254E-06			
34003.932	4.141	0.934E-06	0.239E-06	4.204	0.866E-06	0.221E-06			
34003.982	4.266	0.798E-06	0.202E-06	4.366	0.689E-06	0.173E-06			
34004.032	4.441	0.608E-06	0.152E-06	4.542	0.498E-06	0.123E-06			
34004.082	4.628	0.404E-06	0.984E-07	4.704	0.322E-06	0.774E-07			
34004.132	4.741	0.282E-06	0.672E-07	4.779	0.240E-06	0.567E-07			
34004.182	4.792	0.227E-06	0.533E-07	4.803	0.214E-06	0.501E-07			
34004.232	4.803	0.214E-06	0.501E-07	4.816	0.200E-06	0.467E-07			
34004.282	4.816	0.200E-06	0.467E-07	4.816	0.200E-06	0.467E-07			
34004.332	4.816	0.200E-06	0.467E-07	4.829	0.186E-06	0.433E-07			
34004.382	4.829	0.186E-06	0.433E-07	4.829	0.186E-06	0.433E-07			
34004.432	4.829	0.186E-06	0.433E-07	4.829	0.186E-06	0.433E-07			
34004.482	4.841	0.172E-06	0.399E-07	4.841	0.172E-06	0.399E-07			
34004.532	4.841	0.172E-06	0.399E-07	4.841	0.172E-06	0.399E-07			
34004.582	4.841	0.172E-06	0.399E-07	4.841	0.172E-06	0.399E-07			
34004.632	4.841	0.172E-06	0.399E-07	4.854	0.159E-06	0.365E-07			
34004.682	4.854	0.159E-06	0.365E-07	4.854	0.159E-06	0.365E-07			
34004.732	4.854	0.159E-06	0.365E-07	4.854	0.159E-06	0.365E-07			
34004.782	4.841	0.172E-06	0.399E-07	4.854	0.159E-06	0.365E-07			
34004.832	4.866	0.146E-06	0.334E-07	4.866	0.146E-06	0.334E-07			
34004.882	4.854	0.159E-06	0.365E-07	4.866	0.146E-06	0.334E-07			
34004.932	4.866	0.146E-06	0.334E-07	4.866	0.146E-06	0.334E-07			
34004.982	4.866	0.146E-06	0.334E-07	4.866	0.146E-06	0.334E-07			
34005.032	4.866	0.146E-06	0.334E-07	4.866	0.146E-06	0.334E-07			
34005.082	4.866	0.146E-06	0.334E-07	4.878	0.132E-06	0.301E-07			
34005.132	4.854	0.159E-06	0.365E-07	4.816	0.200E-06	0.467E-07			
34005.182	4.753	0.265E-06	0.637E-07	4.678	0.350E-06	0.844E-07			
34005.232	4.591	0.444E-06	0.109E-06	4.503	0.540E-06	0.134E-06			
34005.282	4.428	0.621E-06	0.155E-06	4.354	0.702E-06	0.177E-06			
34005.332	4.279	0.784E-06	0.199E-06	4.191	0.879E-06	0.225E-06			
34005.382	4.141	0.934E-06	0.239E-06	4.066	0.102E-05	0.261E-06			

Figure 1. Typical Data Sheet



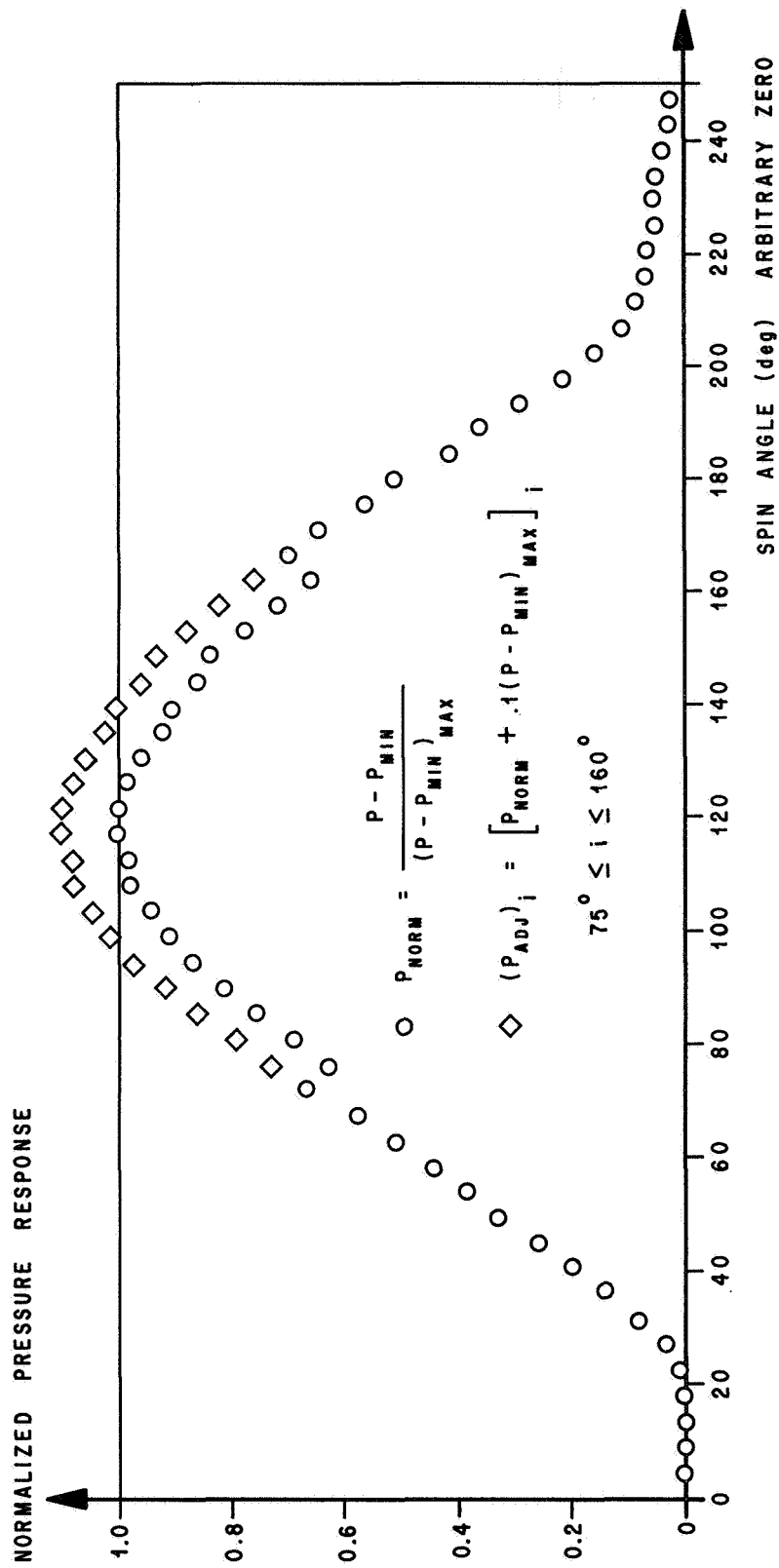


Figure 2. Normalized Pressure Response for Redhead Gauge on Explorer XXXII, Turn-on No. 94, 290 Km Perigee,  $\alpha_{min} = 0^\circ$

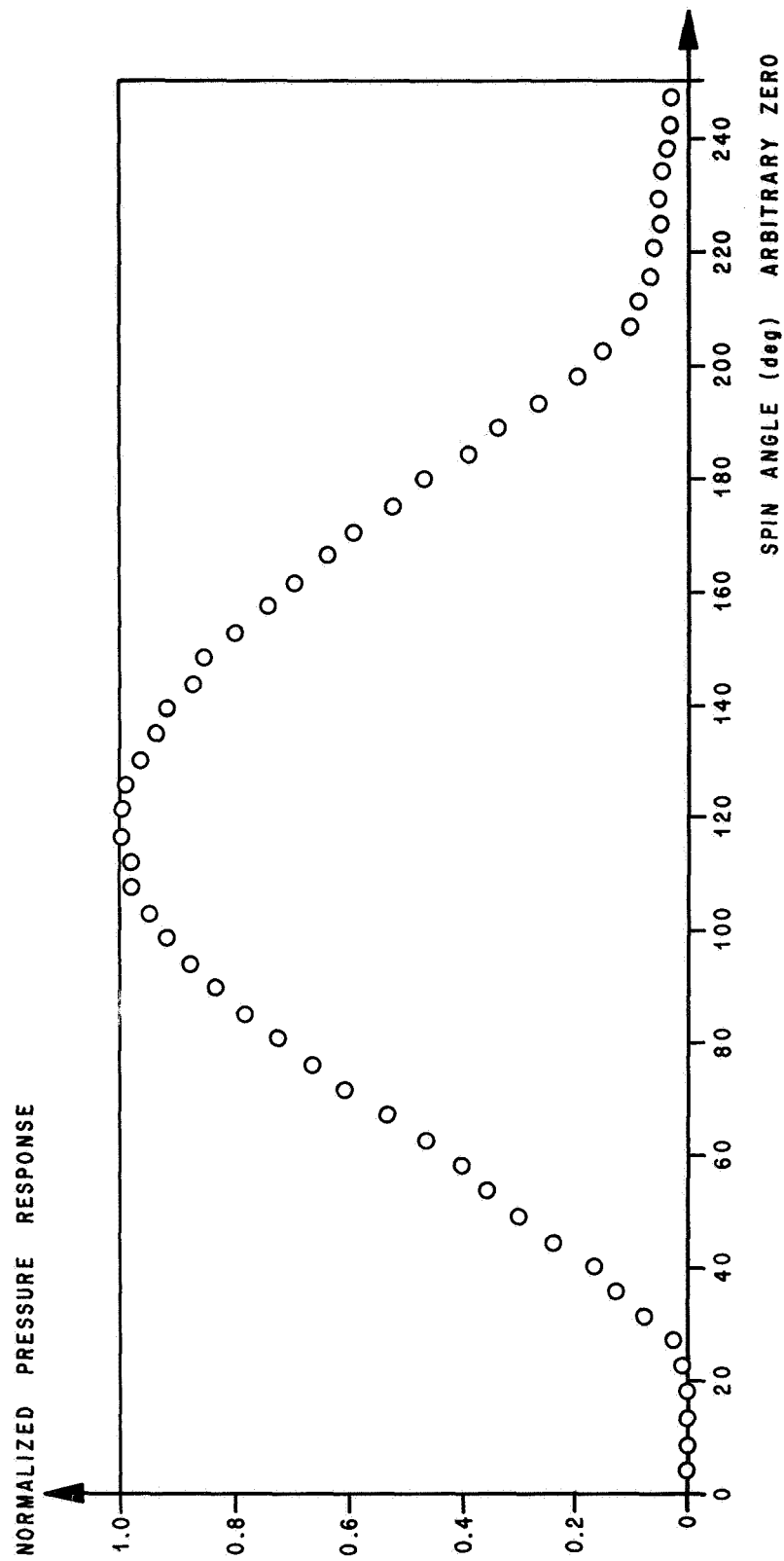


Figure 3. Normalized Adjusted Pressure Response for Redhead Gauge on Explorer XXXII, Turn-on No. 94, 290 Km Perigee,  $C_{min} = 0^\circ$

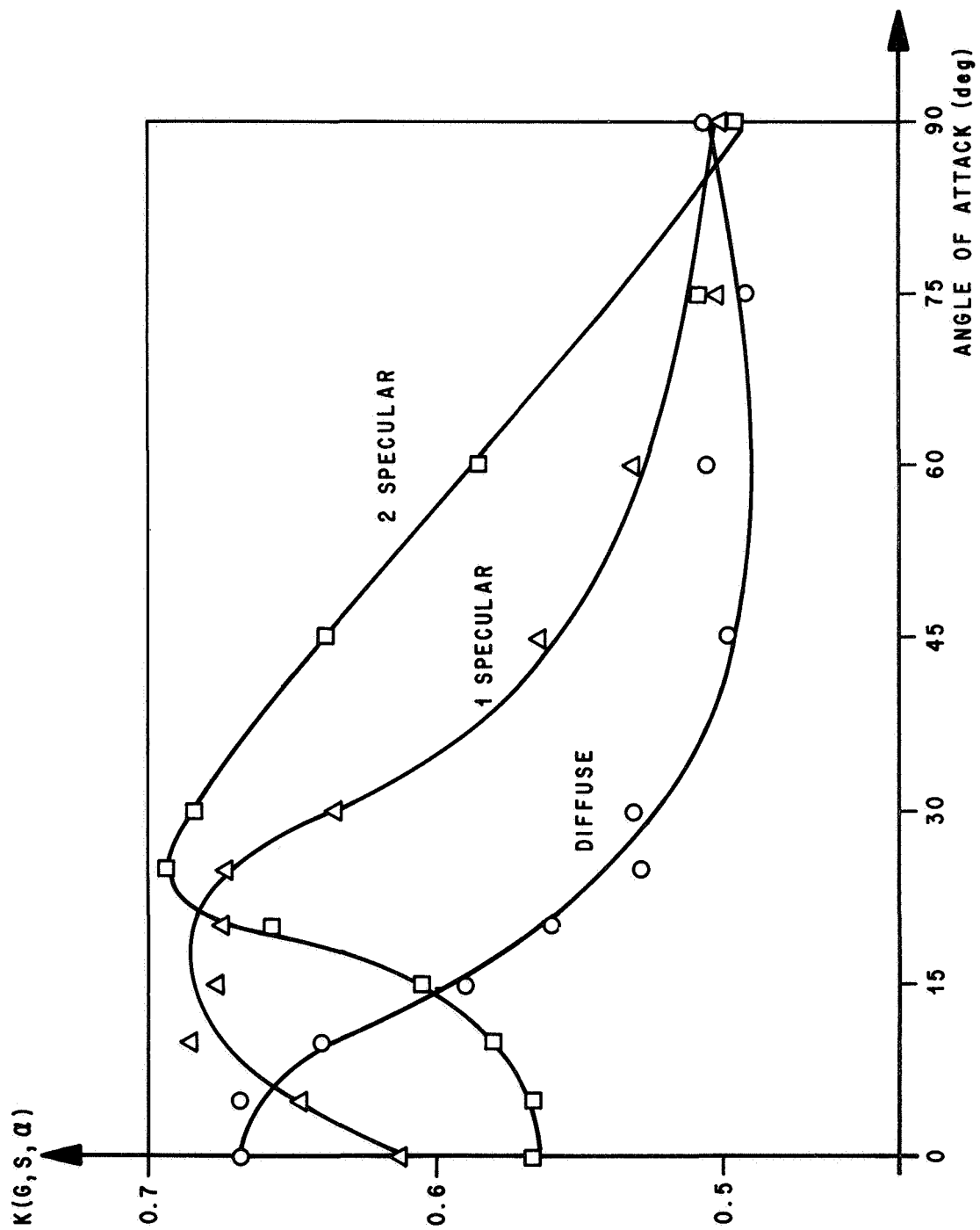


Figure 4. Transmission Probabilities for the Redhead Vacuum Gauge  
on Explorer XXXII, Speed Ratio = 8.0

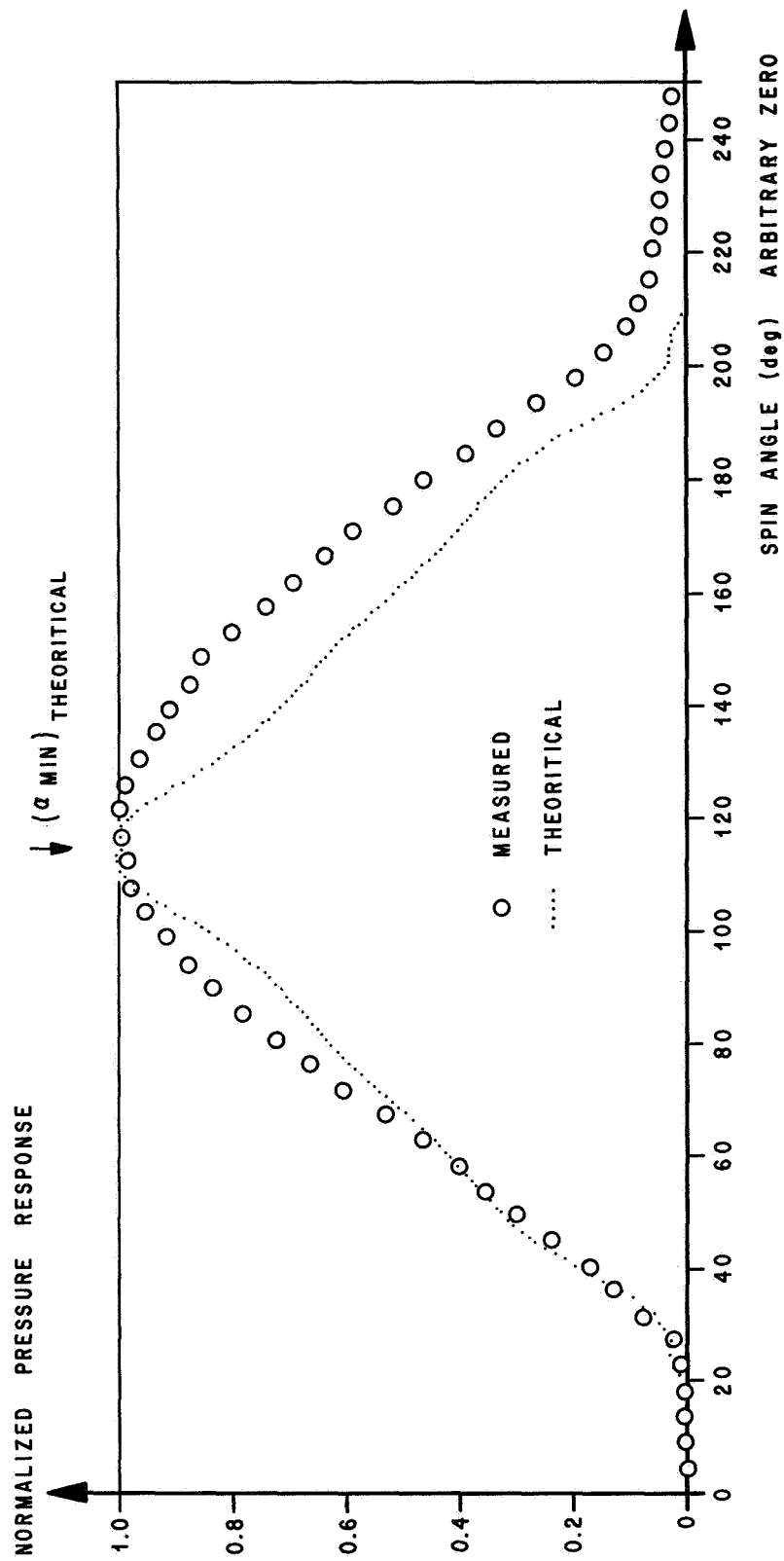


Figure 5. Normalized Adjusted Pressure Response (Measured) Compared to Normalized Theoretical Pressure Response (Predicted using Diffusive Reflections),  $\alpha_{\min} = 0^\circ$

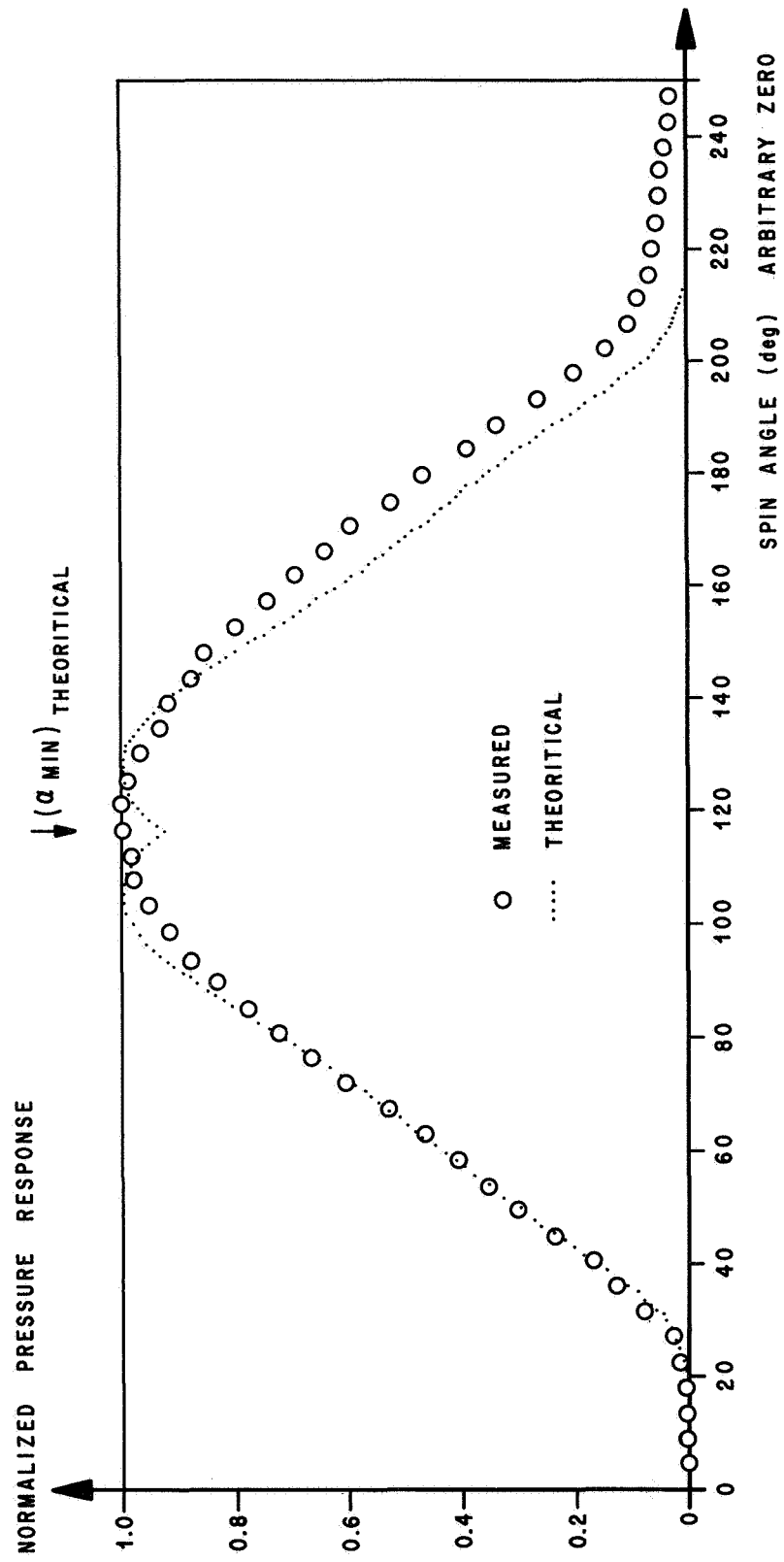


Figure 6. Normalized Adjusted Pressure Response (Measured) Compared to Normalized Theoretical Pressure Response (Predicted using one Specular Reflection),  $\alpha_{\min} = 0^\circ$

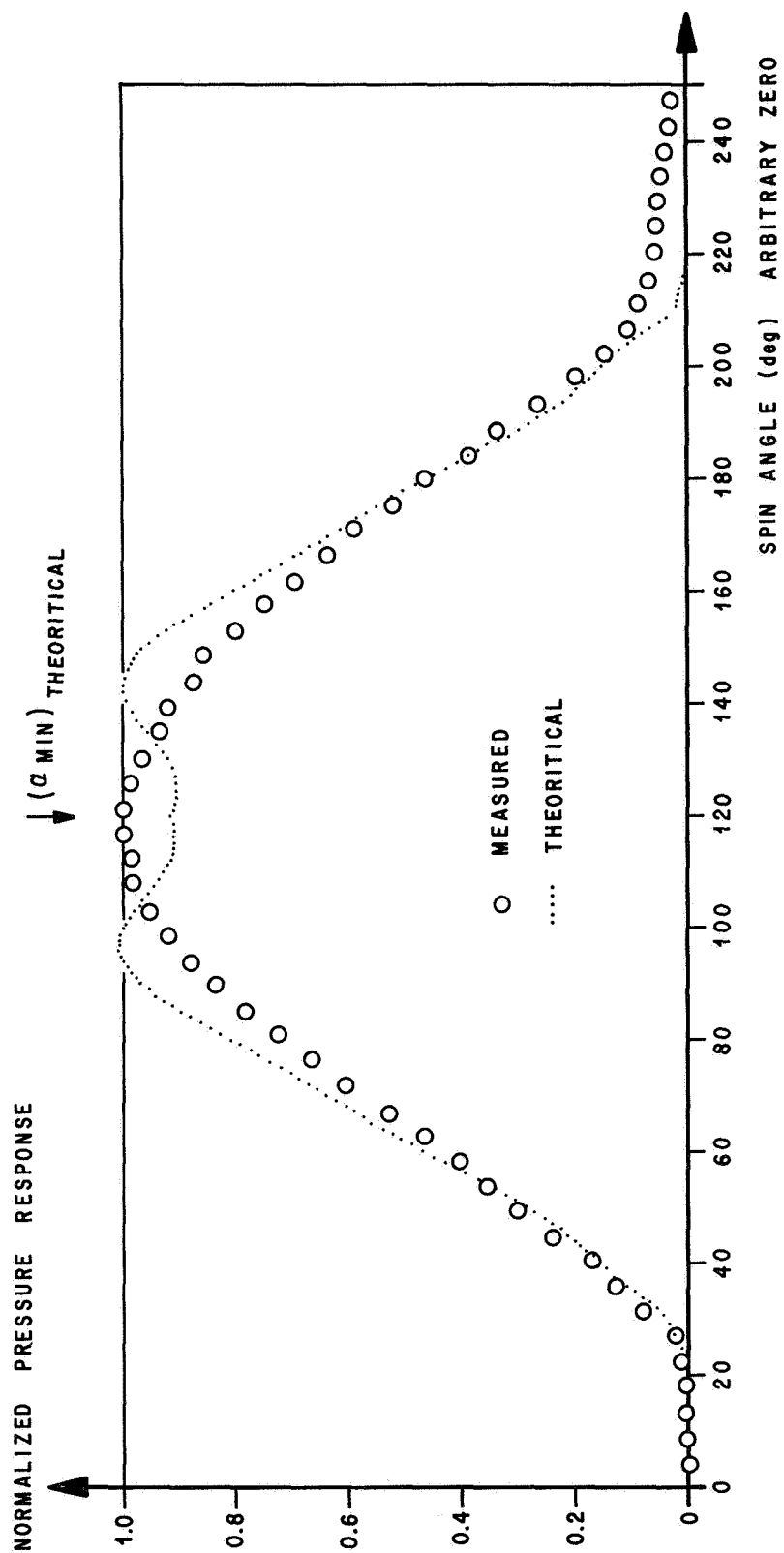


Figure 7. Normalized Adjusted Pressure Response (Measured) Compared to Normalized Theoretical Pressure Response (Predicted using Two Specular Reflections),  $\alpha_{\min} = 0^\circ$

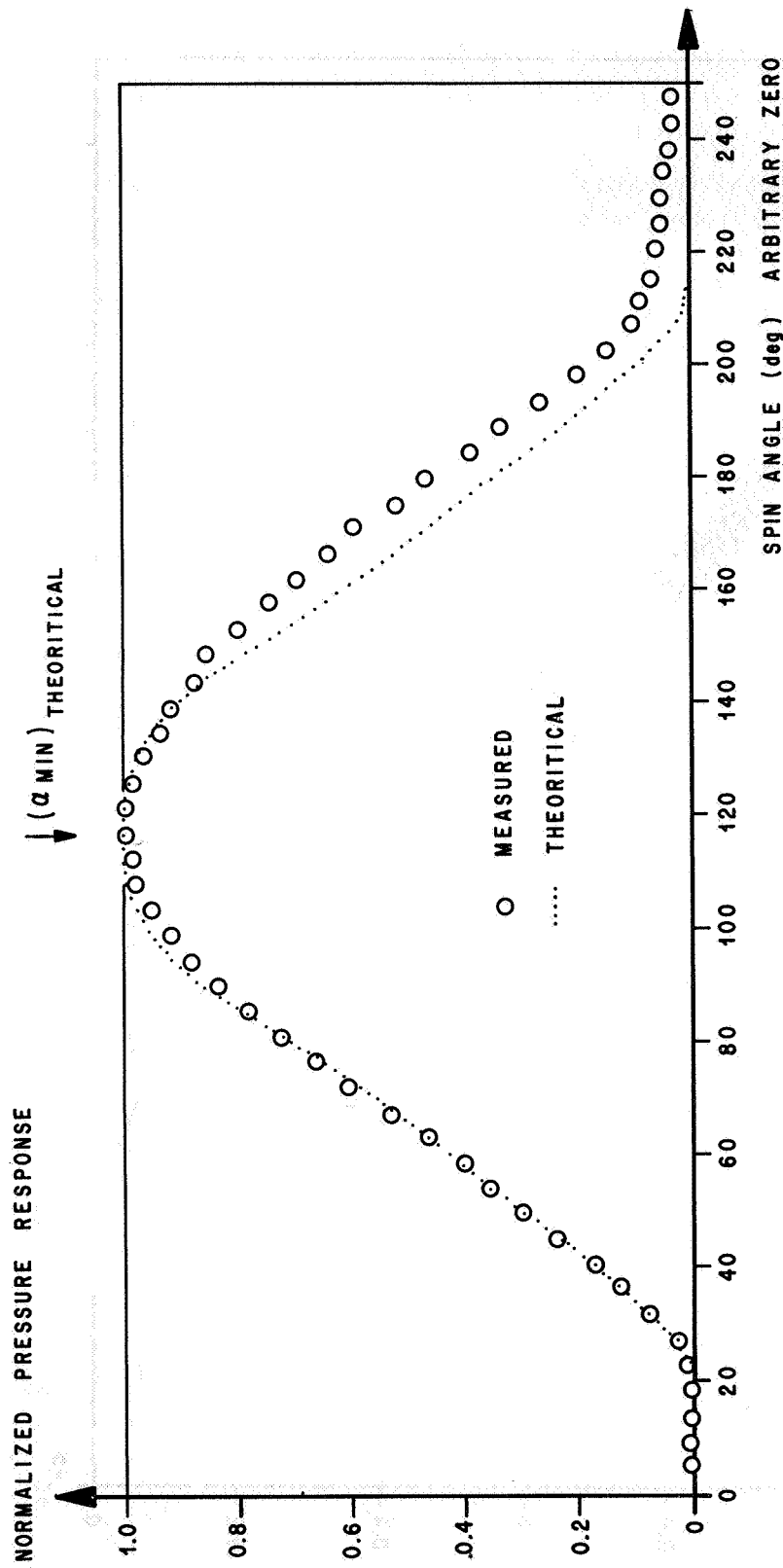


Figure 8. Normalized Adjusted Pressure Response (Measured) Compared to Normalized Theoretical Pressure Response (Predicted using Modified One Specular Reflection Data)  
 $\alpha_{\min} = 0^\circ$

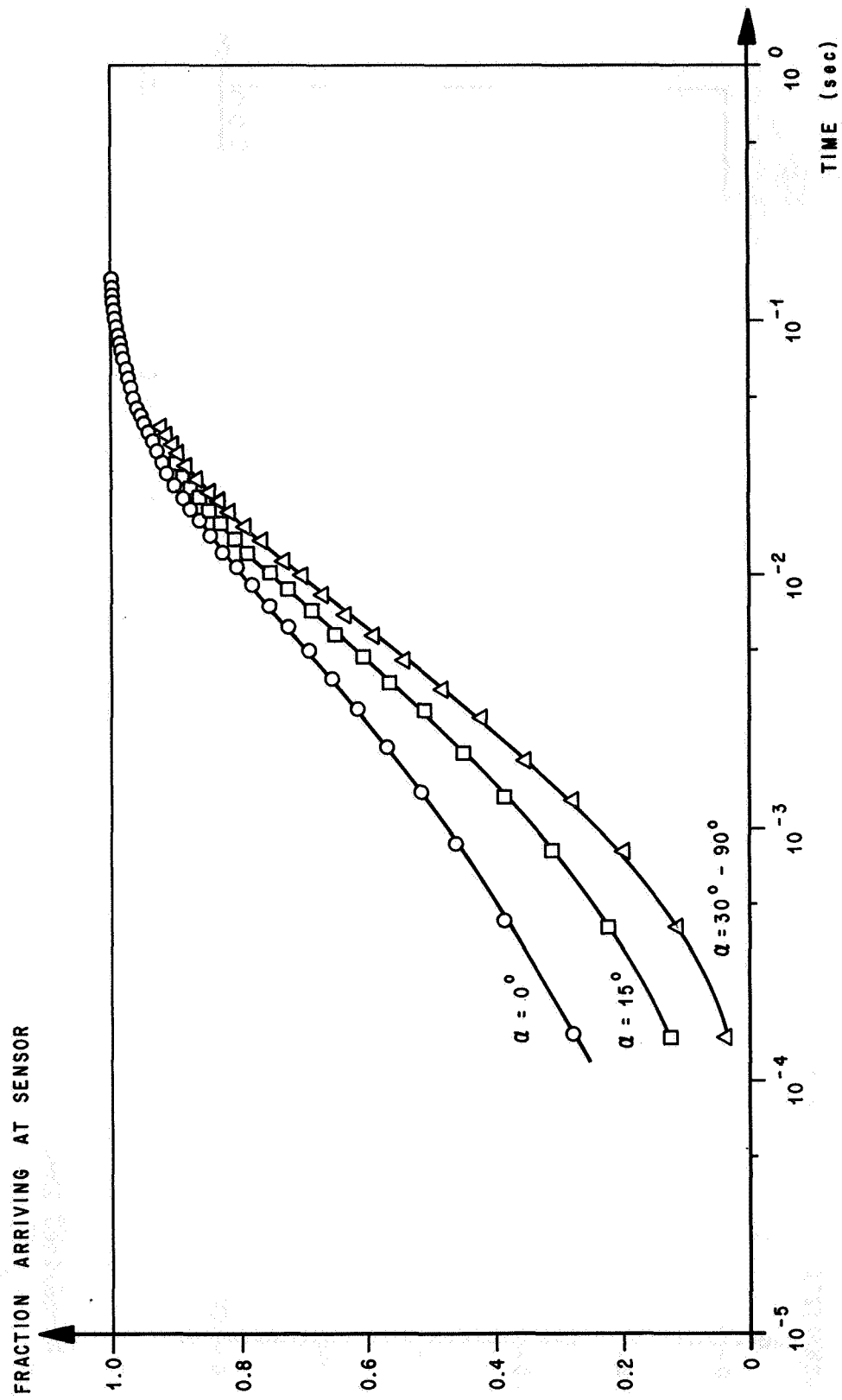


Figure 9. Typical Time Response Characteristics for the Redhead Vacuum Gauge, Speed Ratio = 8, Diffuse Reflection



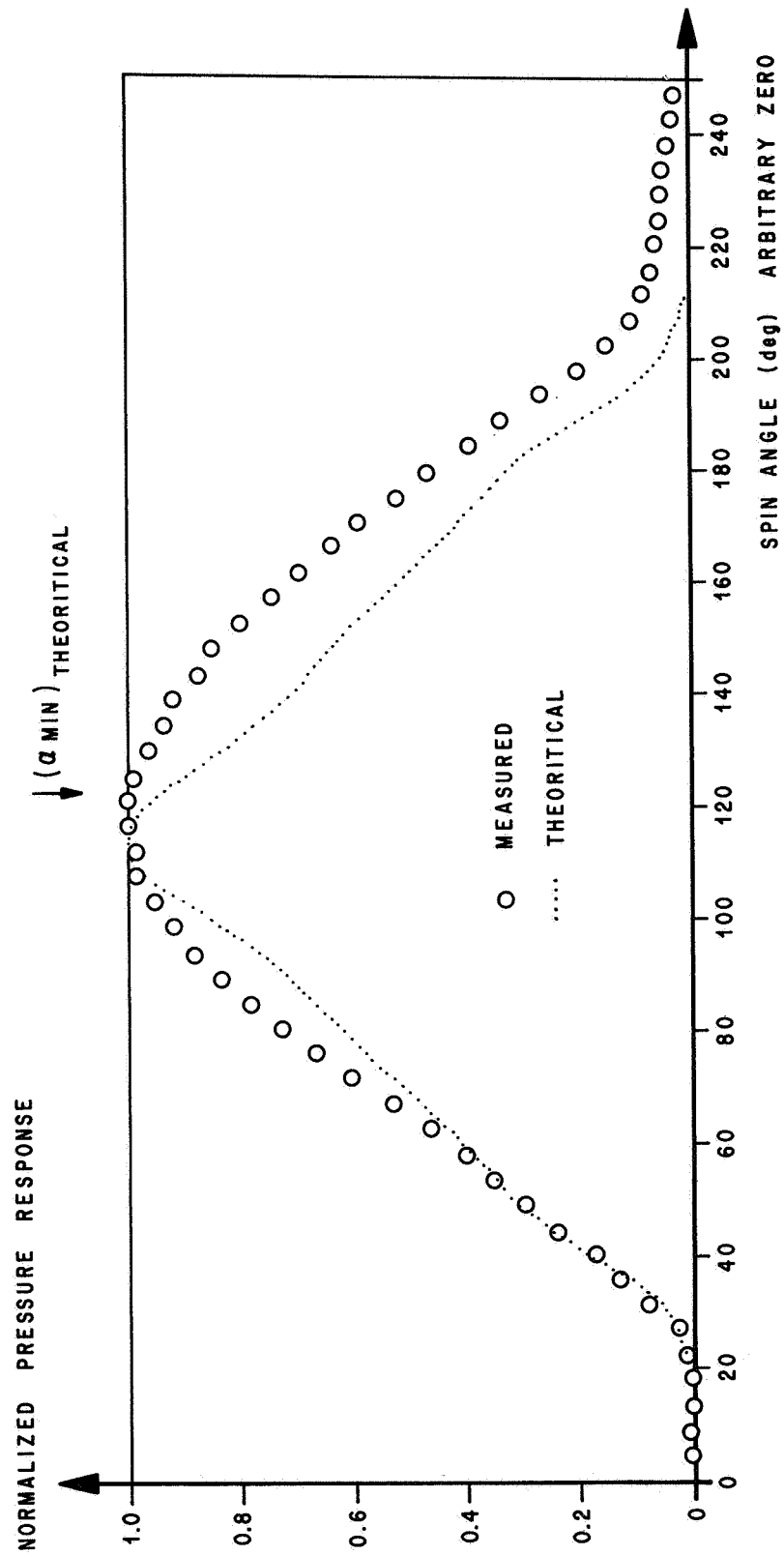


Figure 10. Normalized Adjusted Pressure Response (Measured) Compared to Normalized Theoretical Pressure Response (Predicted using Diffuse Reflections and Time Characteristics)  $\alpha_{min} = 0^\circ$

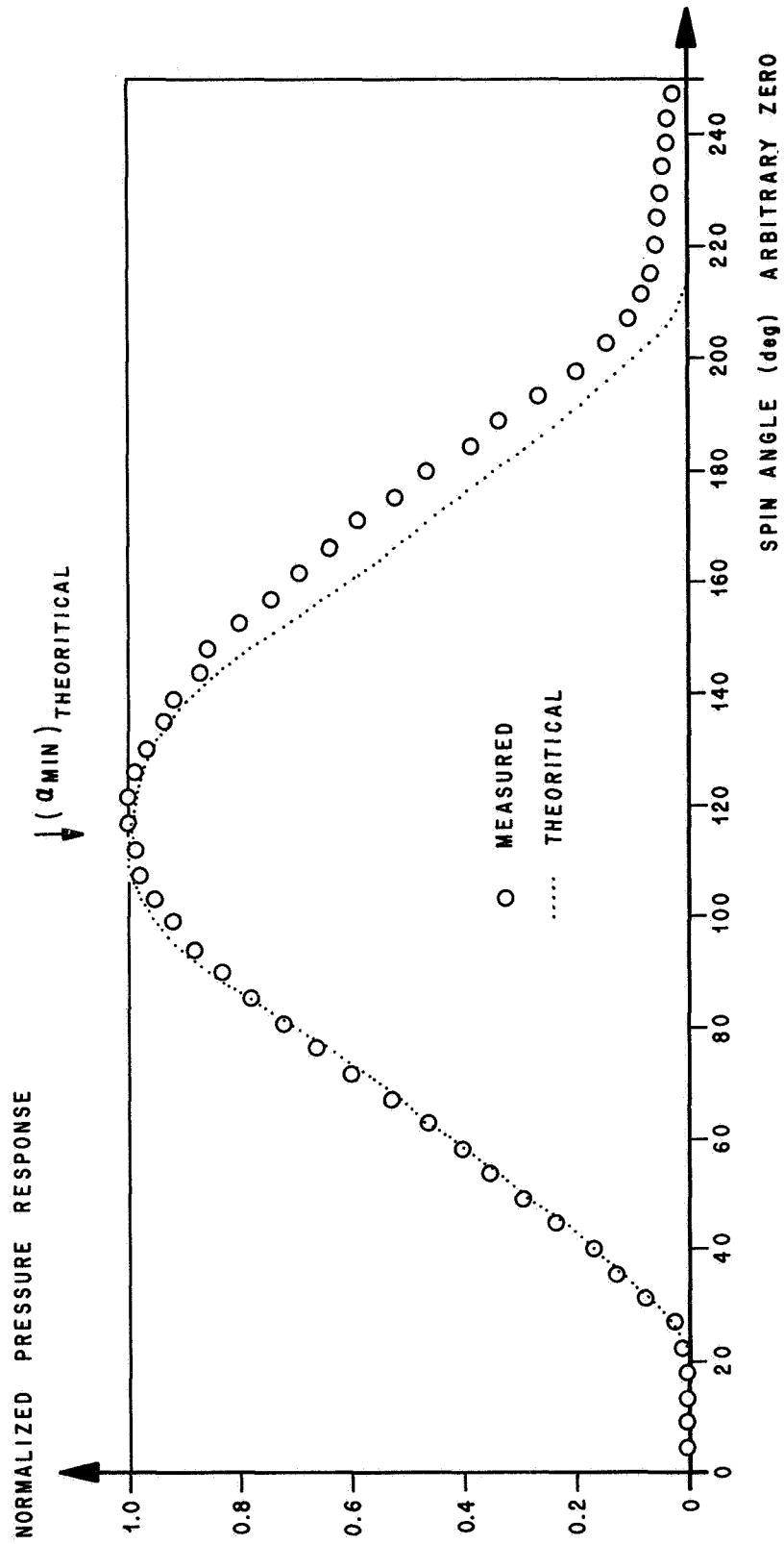


Figure 11. Normalized Adjusted Pressure Response (Measured) Compared to Normalized Theoretical Pressure Response (Predicted using Modified One Specular Reflection and Time Characteristics),  $\alpha_{\min} = 0^\circ$

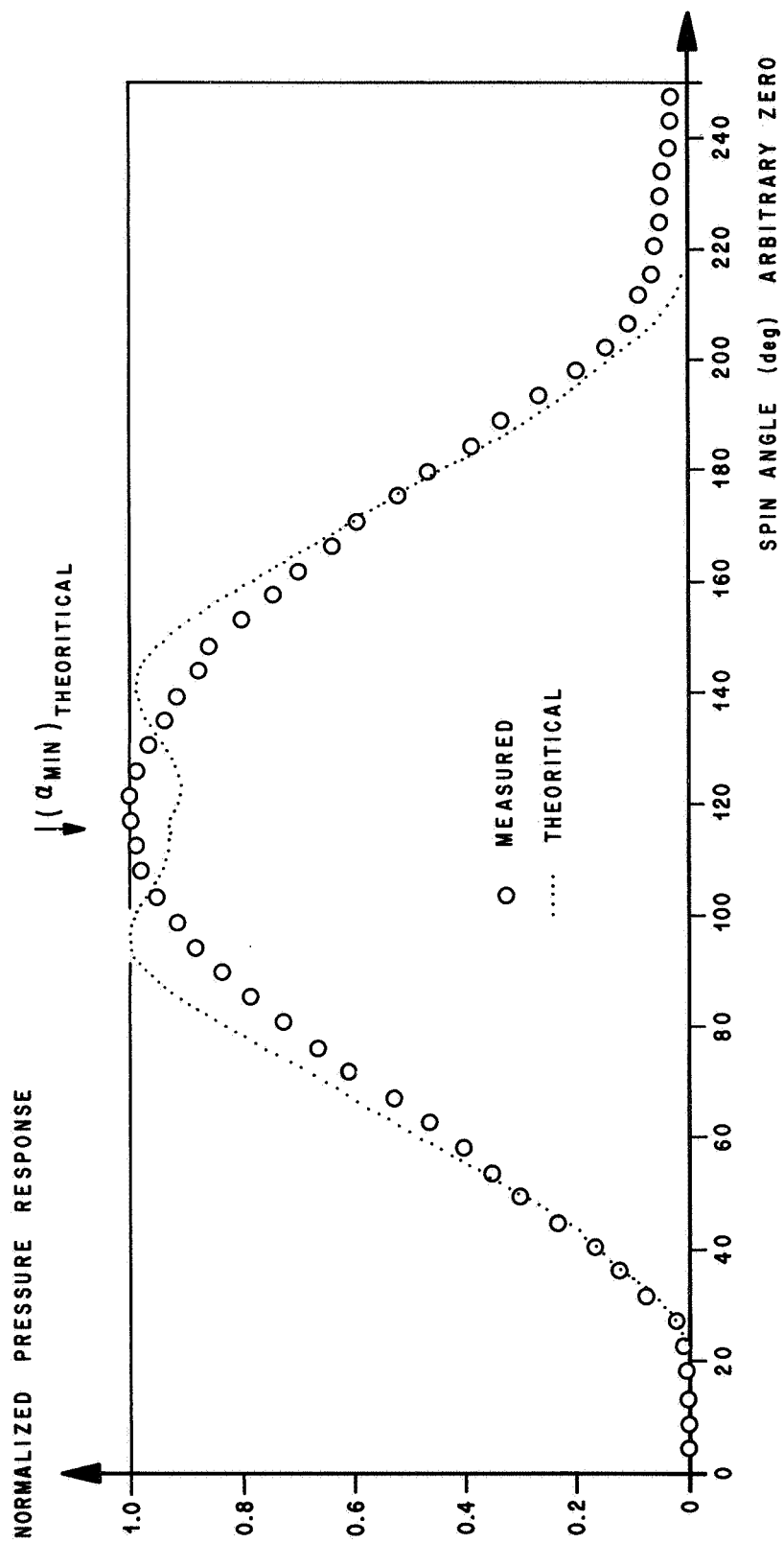


Figure 12. Normalized Adjusted Pressure Response (Measured) Compared to Normalized Theoretical Pressure Response (Predicted using Modified Two Specular Reflection and Time Characteristics),  $\alpha_{\min} = 0^\circ$ .

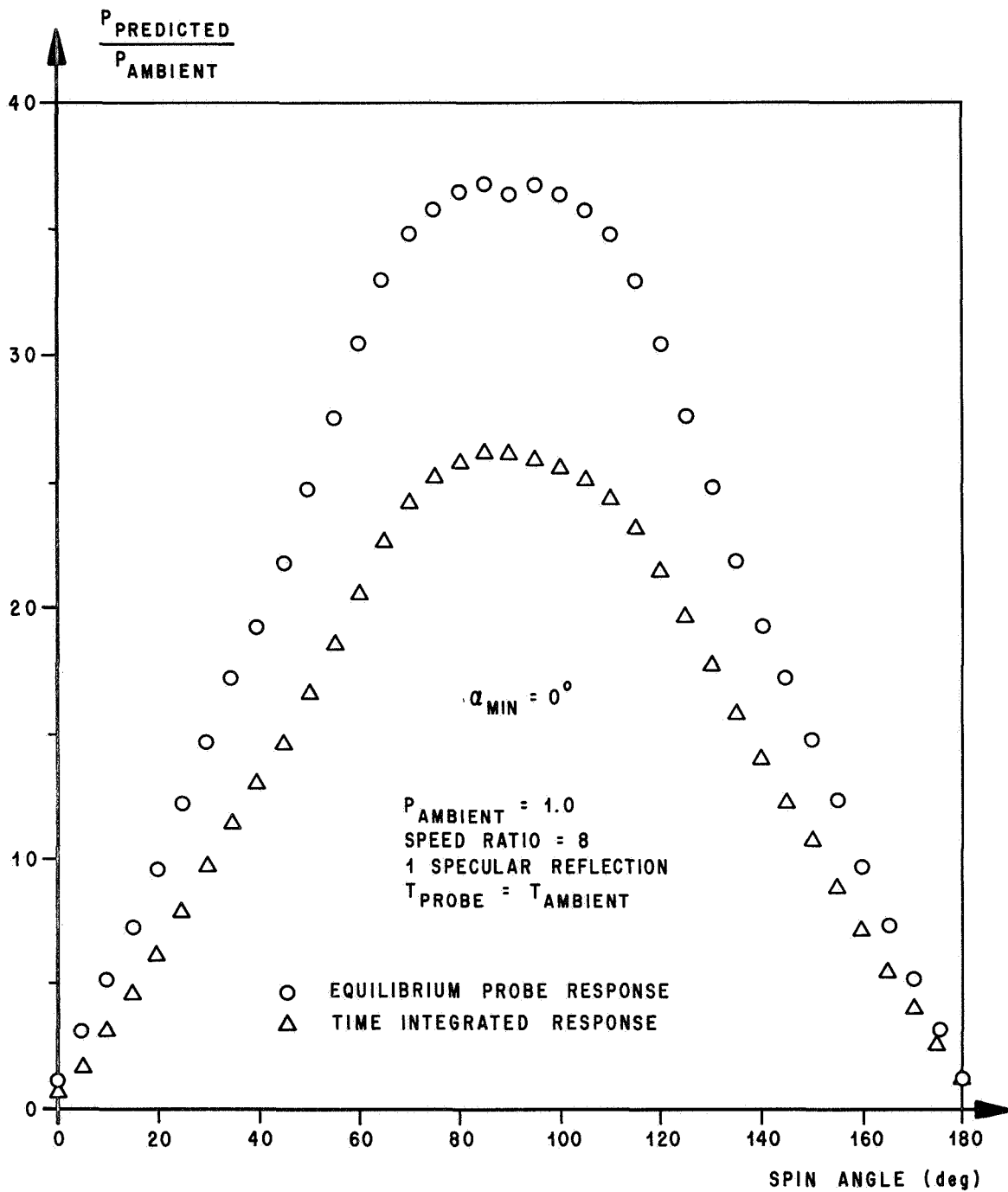


Figure 13. Pressure Response Characteristics for the Redhead Gauge For Equilibrium Conditions and Time Delayed Conditions

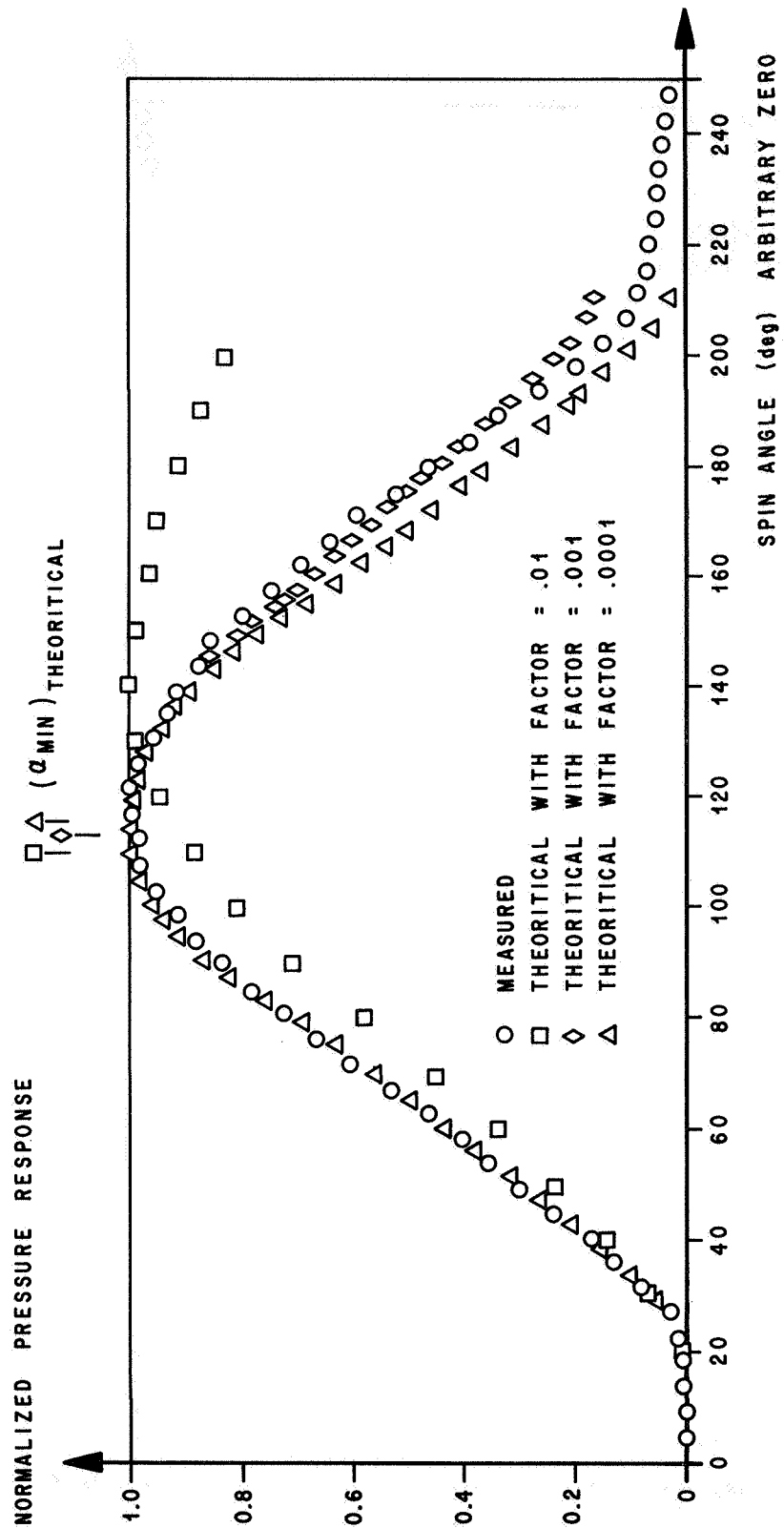


Figure 14. Normalized Adjusted Pressure Response (Measured) Compared with Normalized Theoretical Pressure Response (Predicted using Modified One Specular Reflection Data, Time Characteristics, and Factors of .01, .001, and .0001 of the Total Integrated Density),  $\alpha_{\min} = 0^\circ$ .

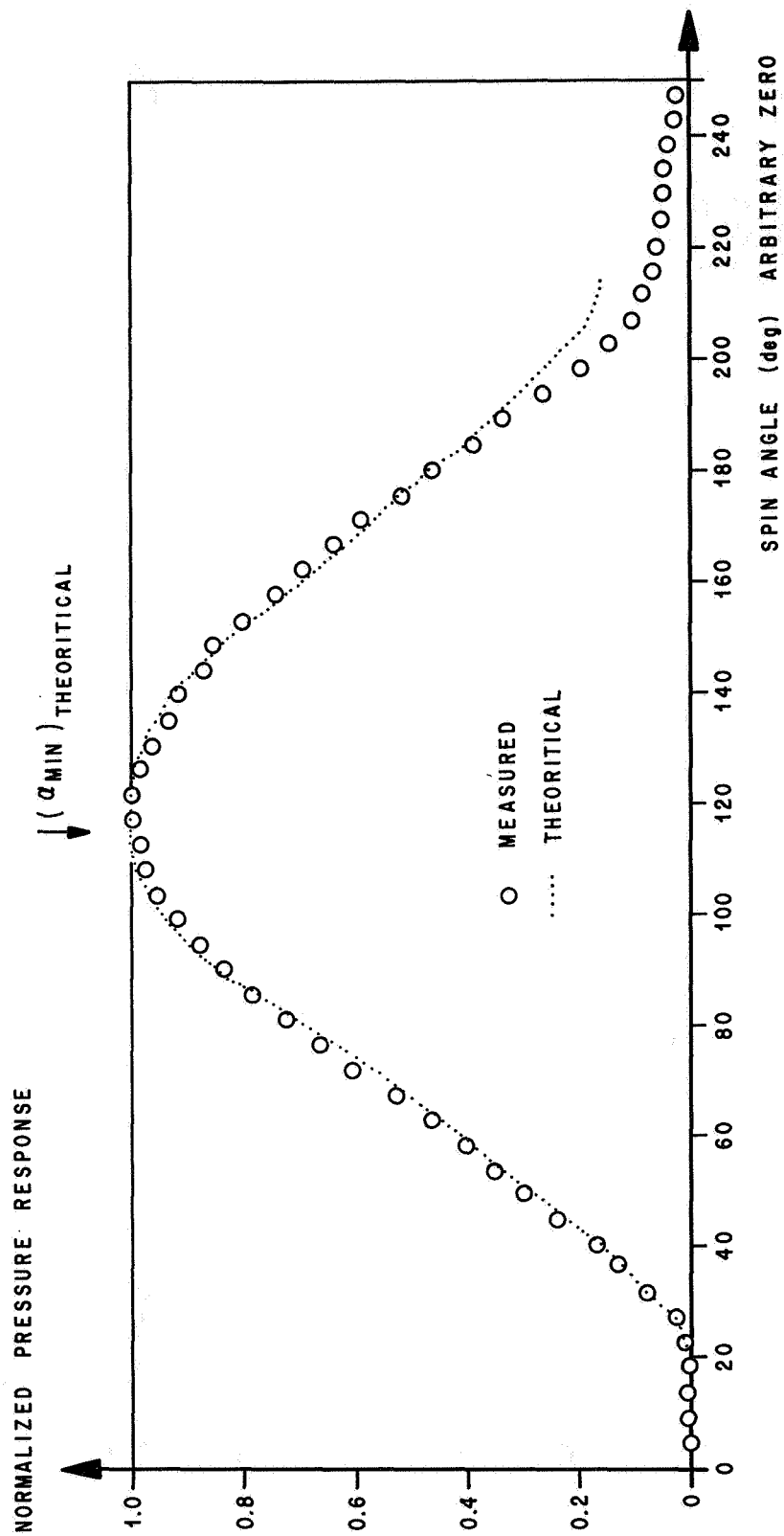


Figure 15. Normalized Adjusted Pressure Response (Measured) Compared to Normalized Theoretical Pressure Response (Predicted using Modified One Specular Reflection Data, Time Characteristics, and with a factor of .001 of the Total Integrated Density)  
 $\alpha_{\min} = 0^\circ$ .

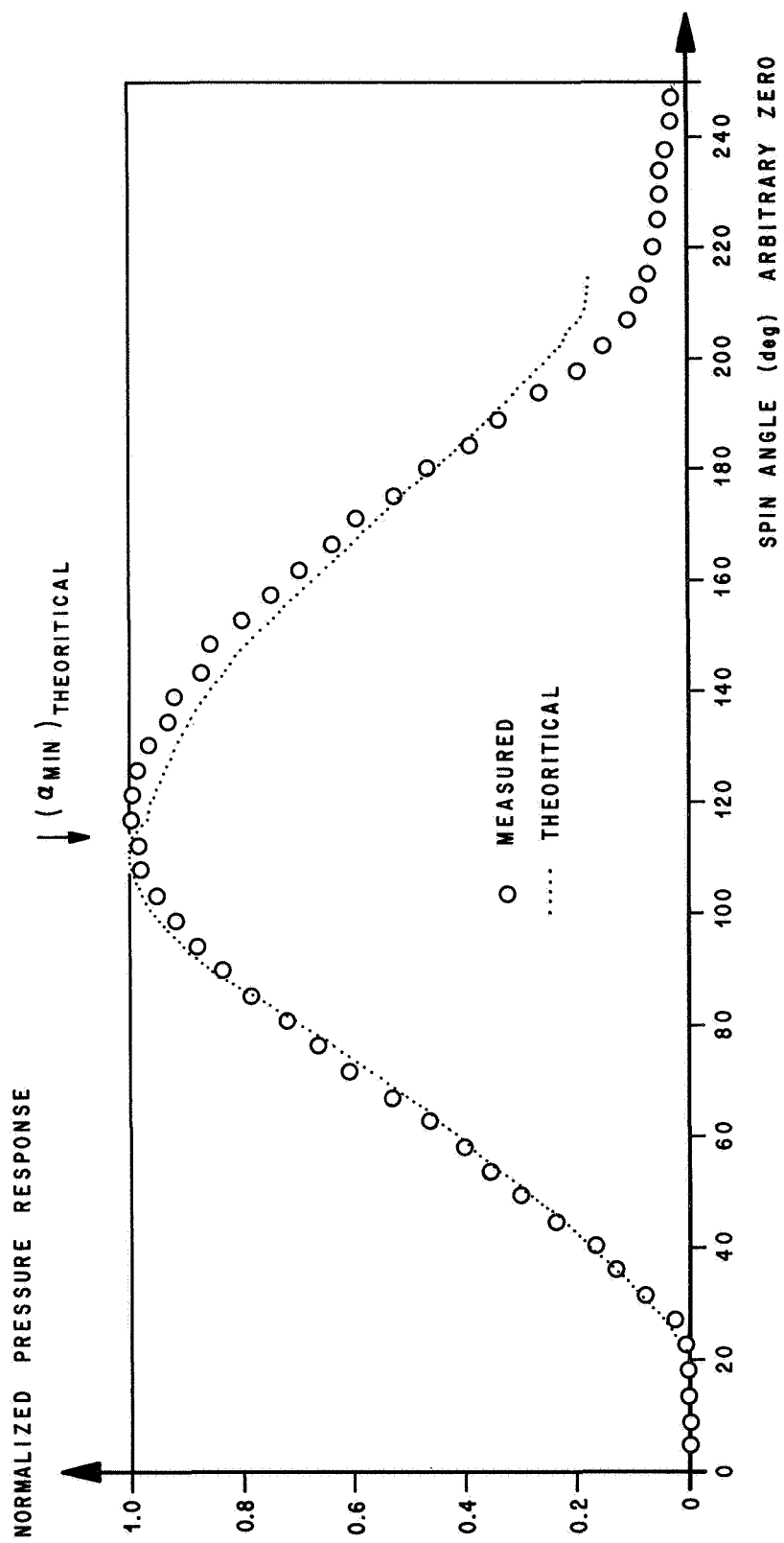


Figure 16. Normalized Adjusted Pressure Response (Measured) Compared to Normalized Theoretical Pressure Response (Predicted using Modified One Specular Reflection Data, Time Characteristics, and with a factor of .001 of the Total Integrated Density),  $\alpha_{\min} = 0^\circ$ , Spin Rate = 1.5 cycles/sec.

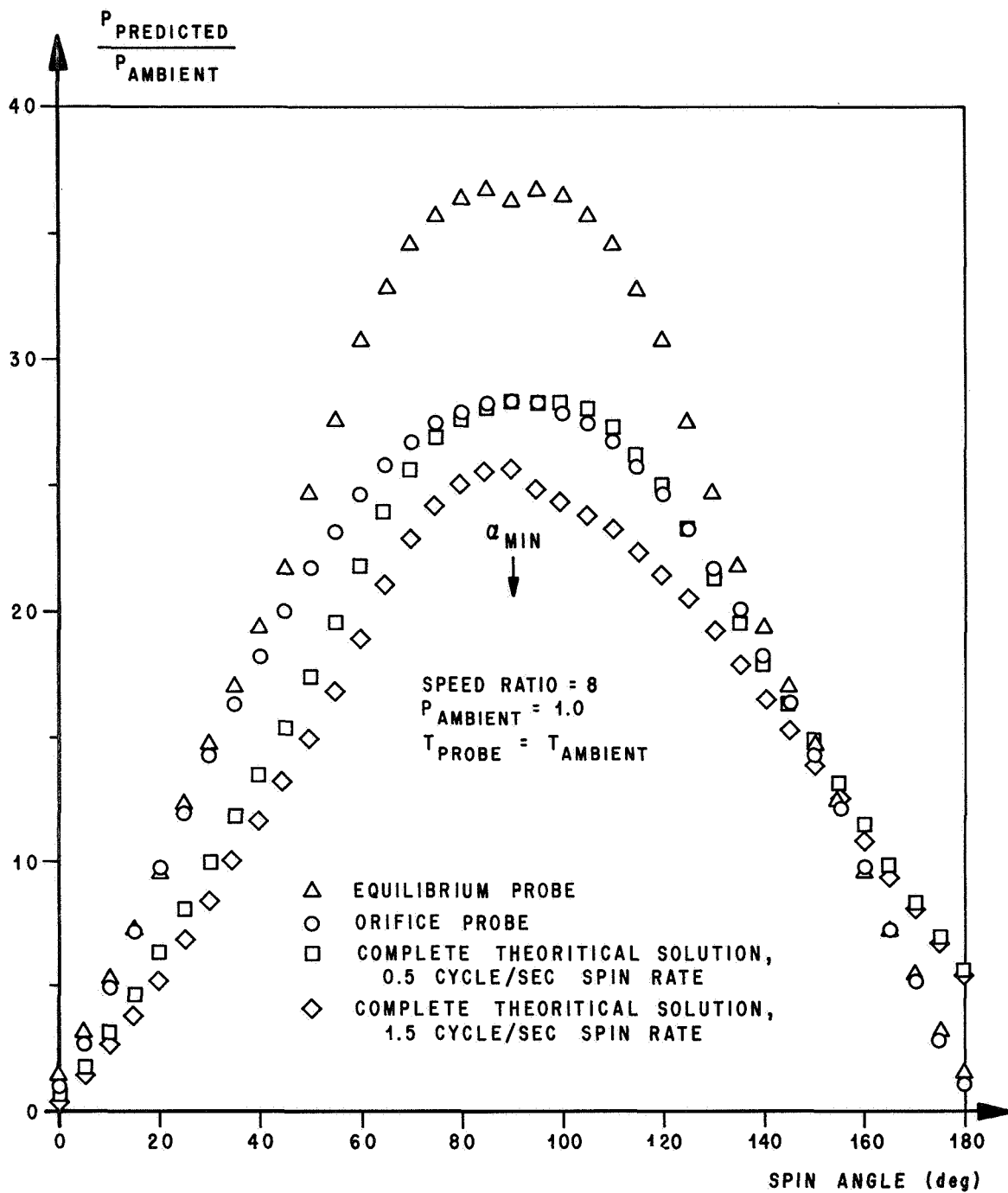


Figure 17. Pressure Response Characteristics for the Redhead Gauge  
 For Various Modes of Interpretation,  $\alpha_{\text{min}} = 0^\circ$



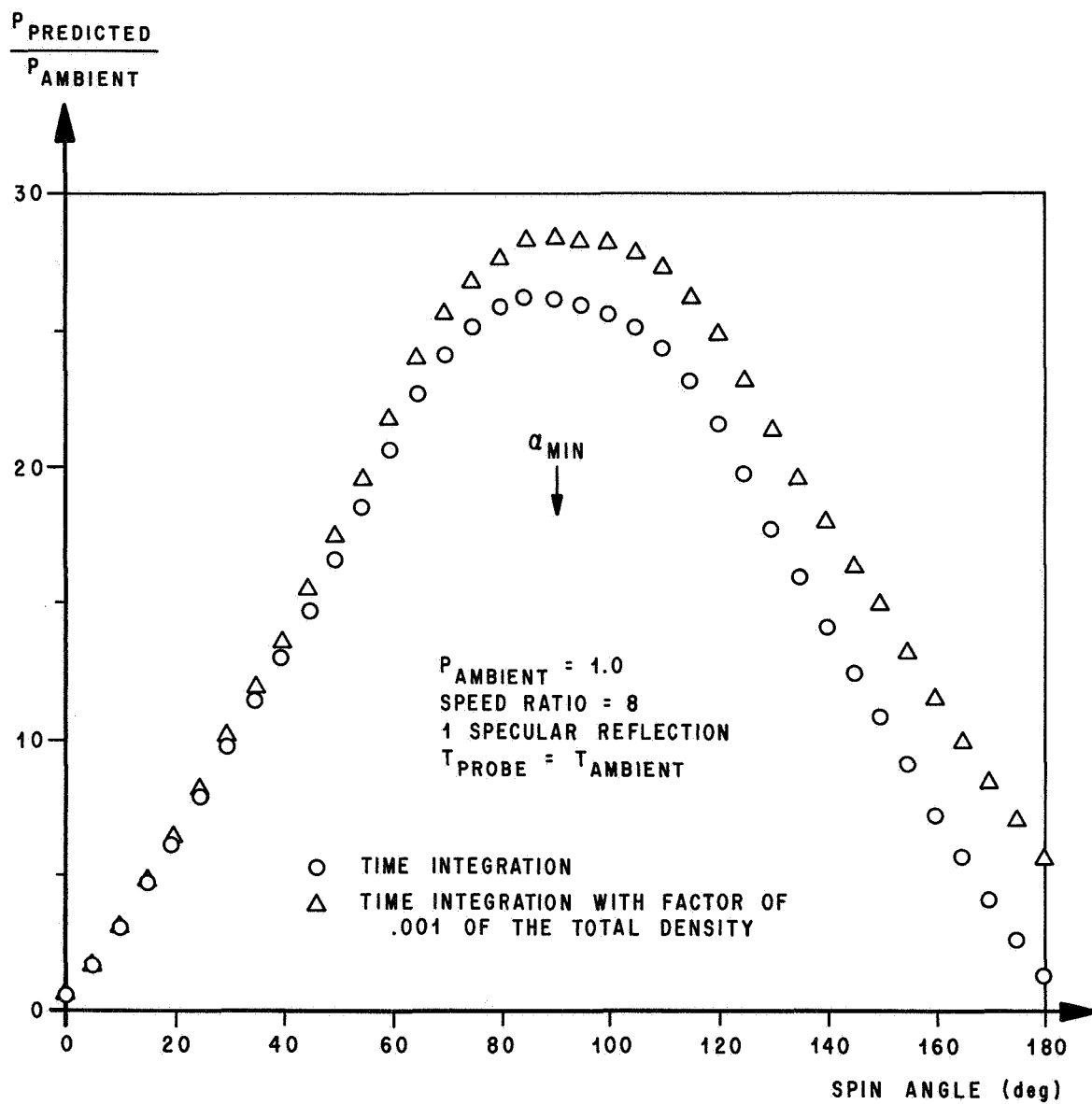


Figure 18. Pressure Response Characteristics for the Redhead Gauge  
 $\alpha_{\text{min}} = 0^\circ$

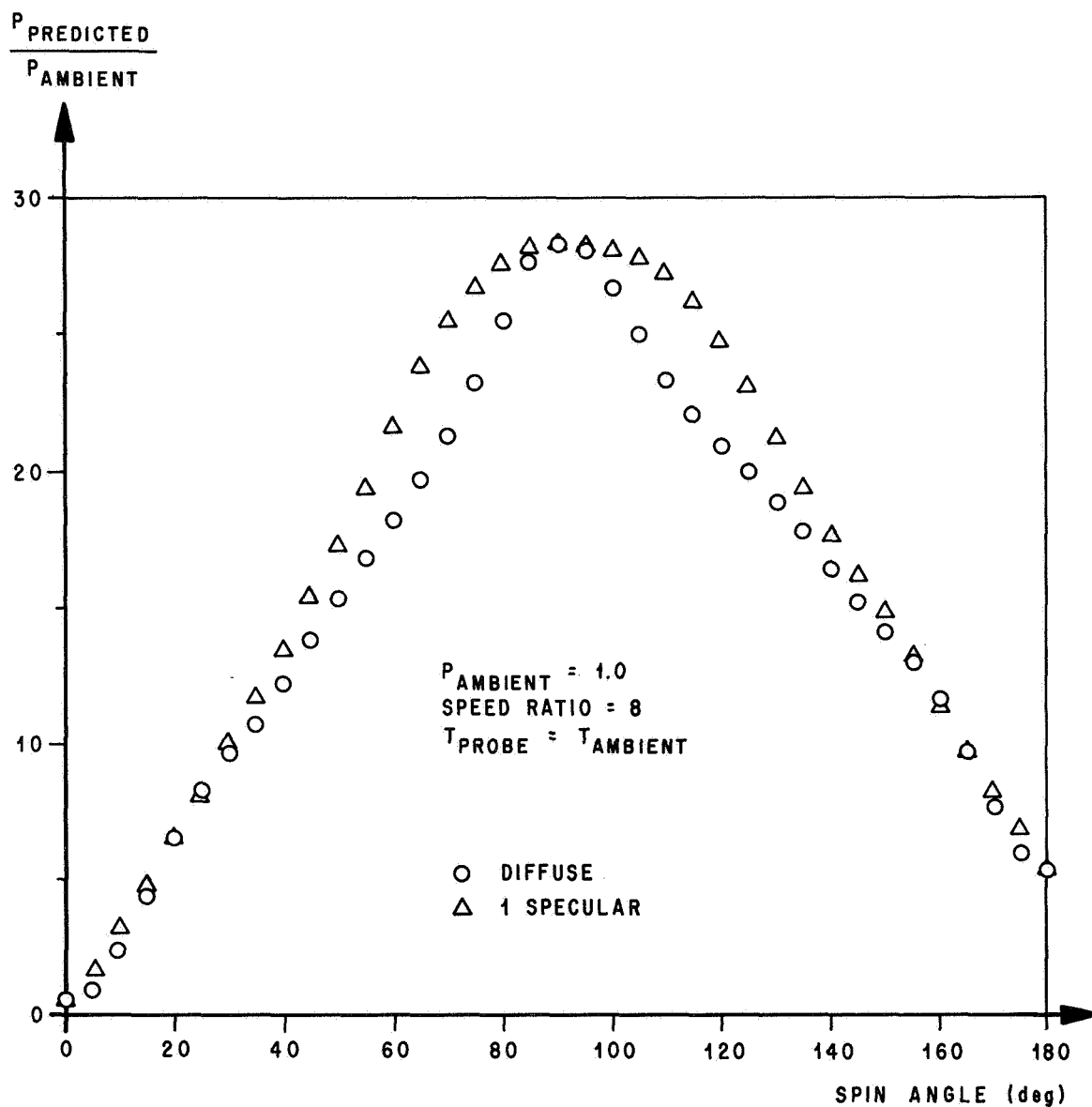


Figure 19. Pressure Response Characteristics for the Redhead Gauge For Diffuse Reflections and One Specular Reflection, Both with Time Characteristics and a Factor of .001 of the Density  $\alpha_{\text{min}} = 0^\circ$ .

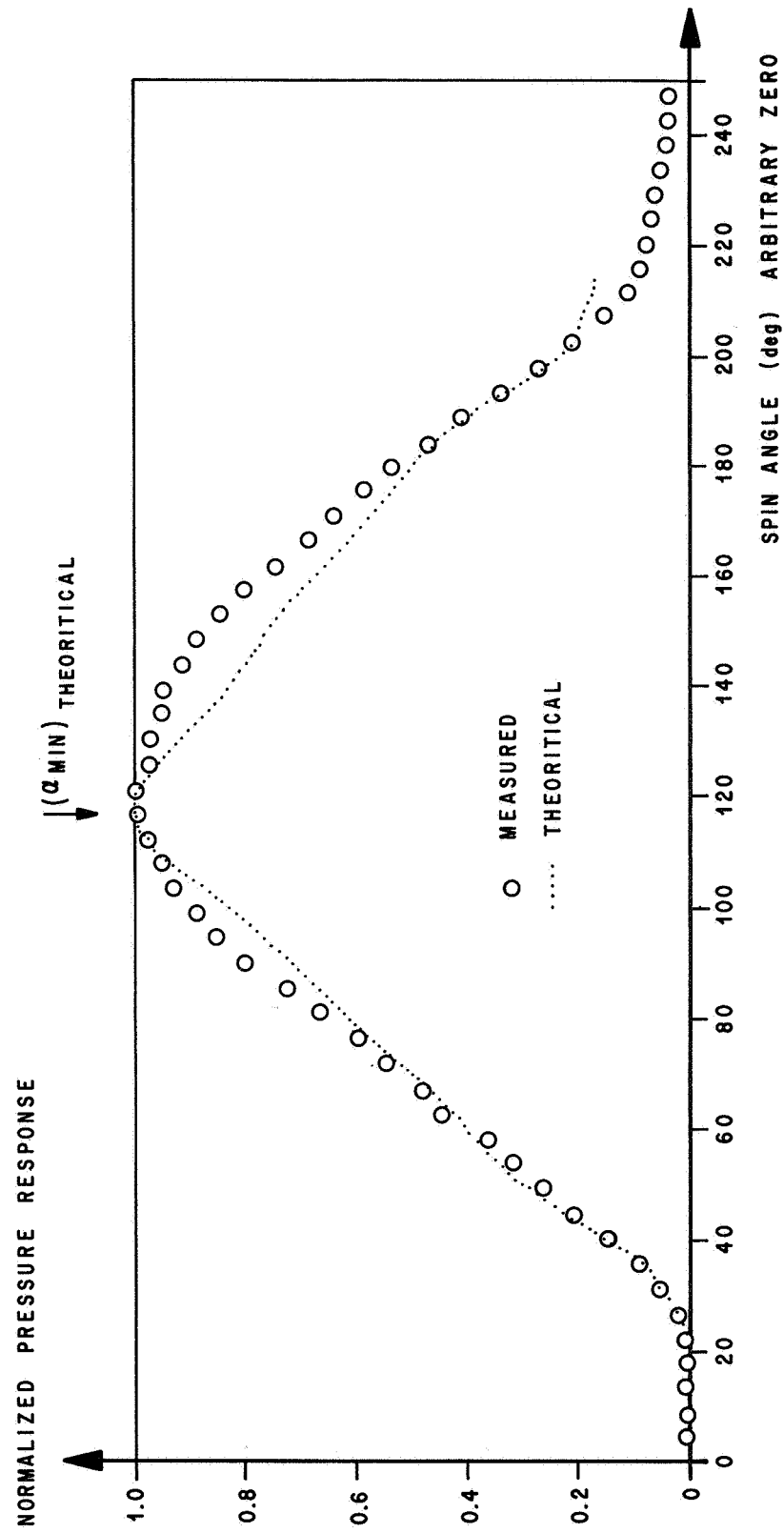


Figure 20. Normalized Adjusted Pressure Response (Measured) Compared to Normalized Theoretical Pressure Response (Predicted using Diffuse Reflections, Time Characteristics, and a Factor of .001 of the Total Number Density),  $\alpha_{\min} = 10^\circ$ .

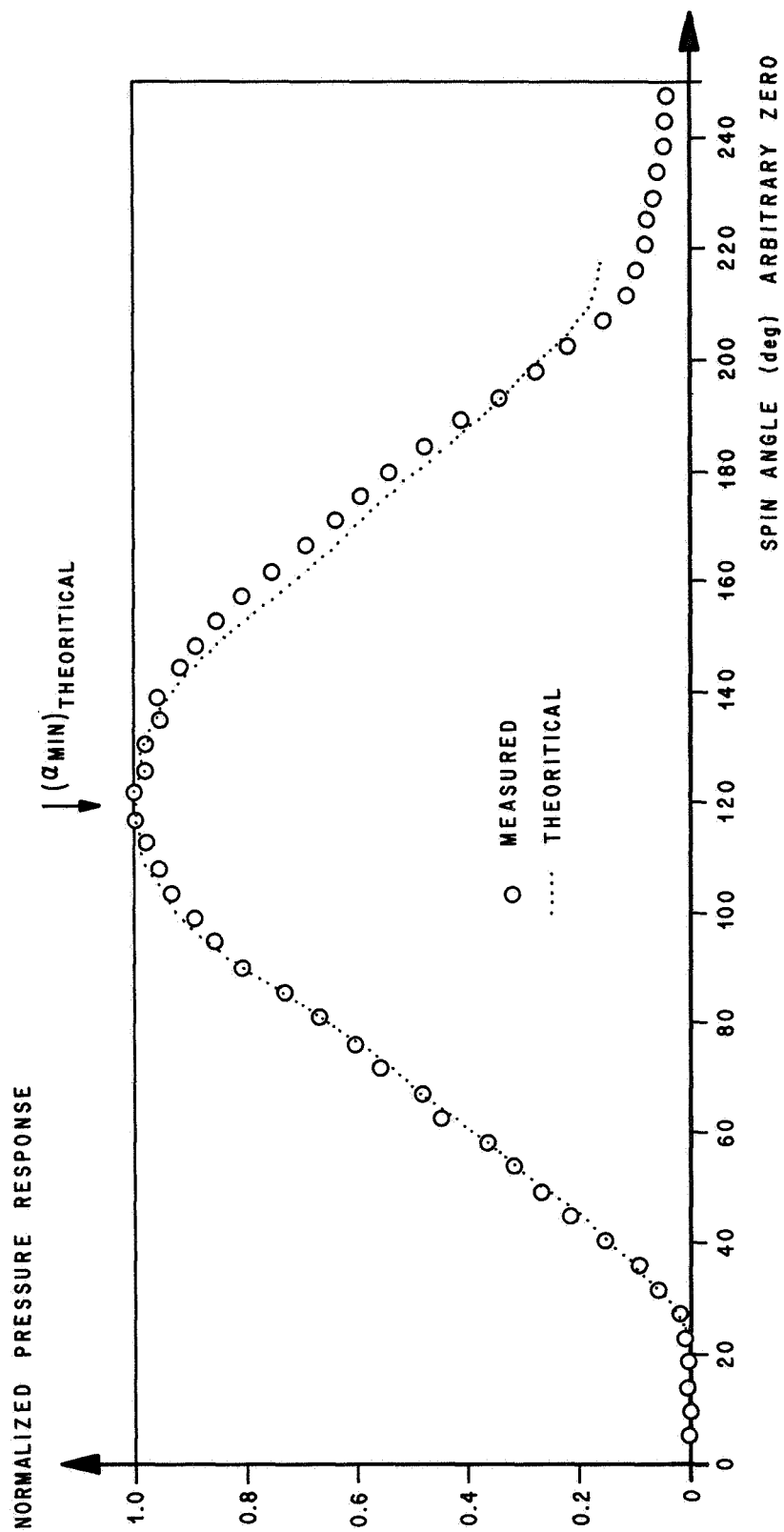


Figure 21. Normalized Adjusted Pressure Response (Measured) Compared to Normalized Theoretical Pressure Response (Predicted using Modified One Specular Reflection Data, Time Characteristics, and a Factor of .001 of the Total Number Density),  $\alpha_{min} = 10^\circ$ .

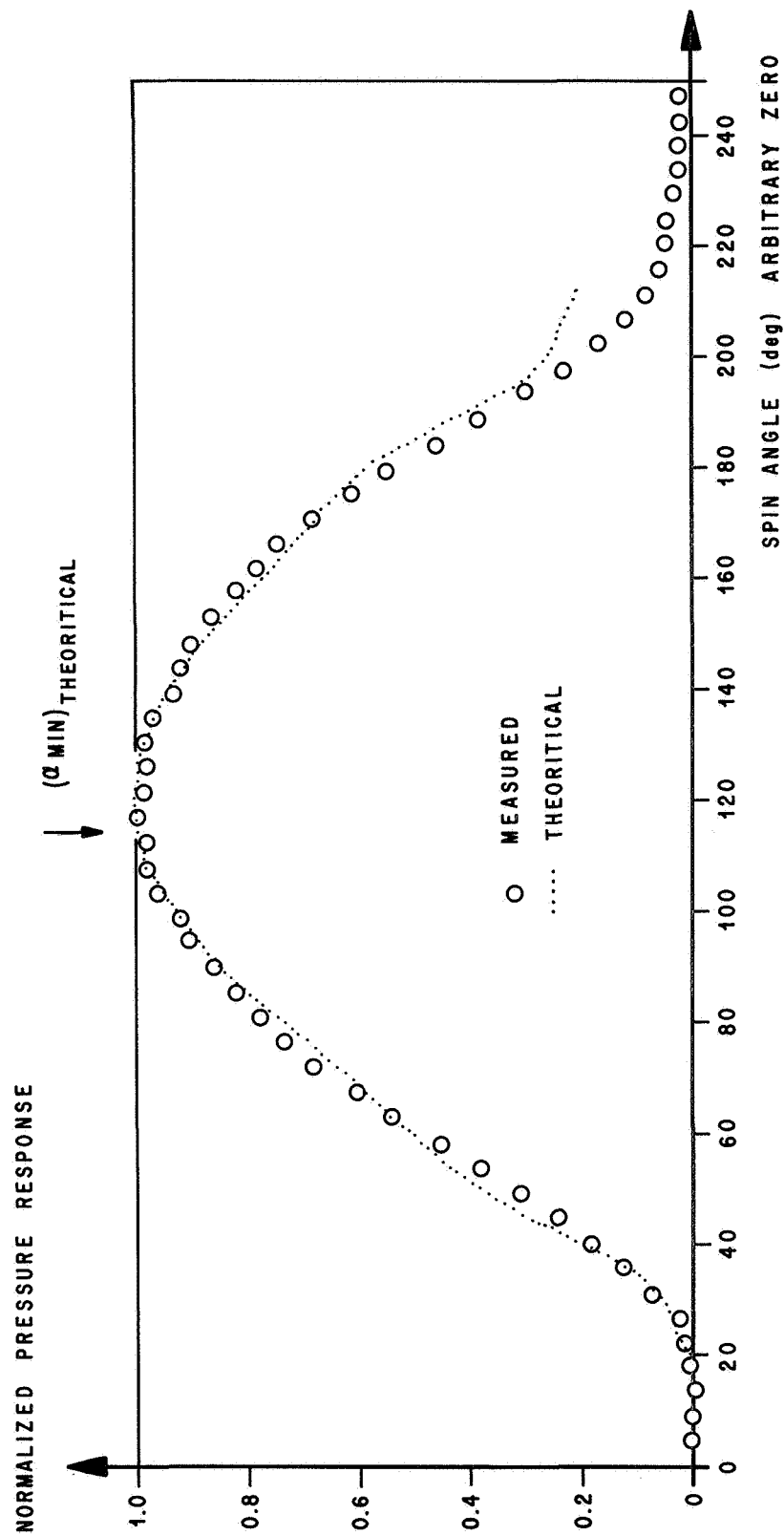


Figure 22. Normalized Adjusted Pressure Response (Measured) Compared to Normalized Theoretical Pressure Response (Predicted using Diffuse Reflections, Time Characteristics, and a Factor of .001 of the Total Number Density),  $\alpha_{\min} = 30^\circ$ .

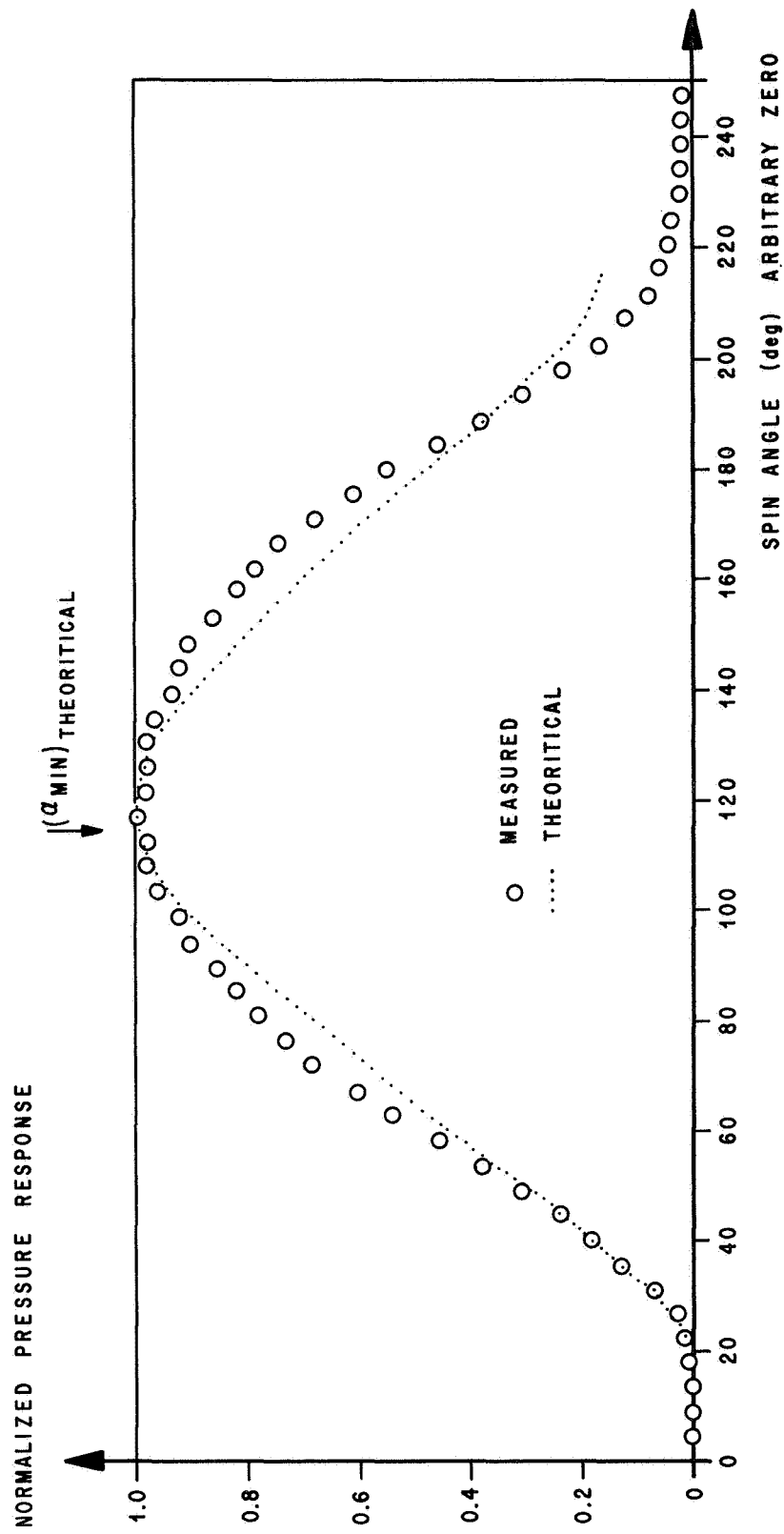


Figure 23. Normalized Adjusted Pressure Response (Measured) Compared to Normalized Theoretical Pressure Response (Predicted using Modified One Specular Reflection Data, Time Characteristics, and a Factor of .001 of the Total Number Density),  $\alpha_{\min} = 30^\circ$ .

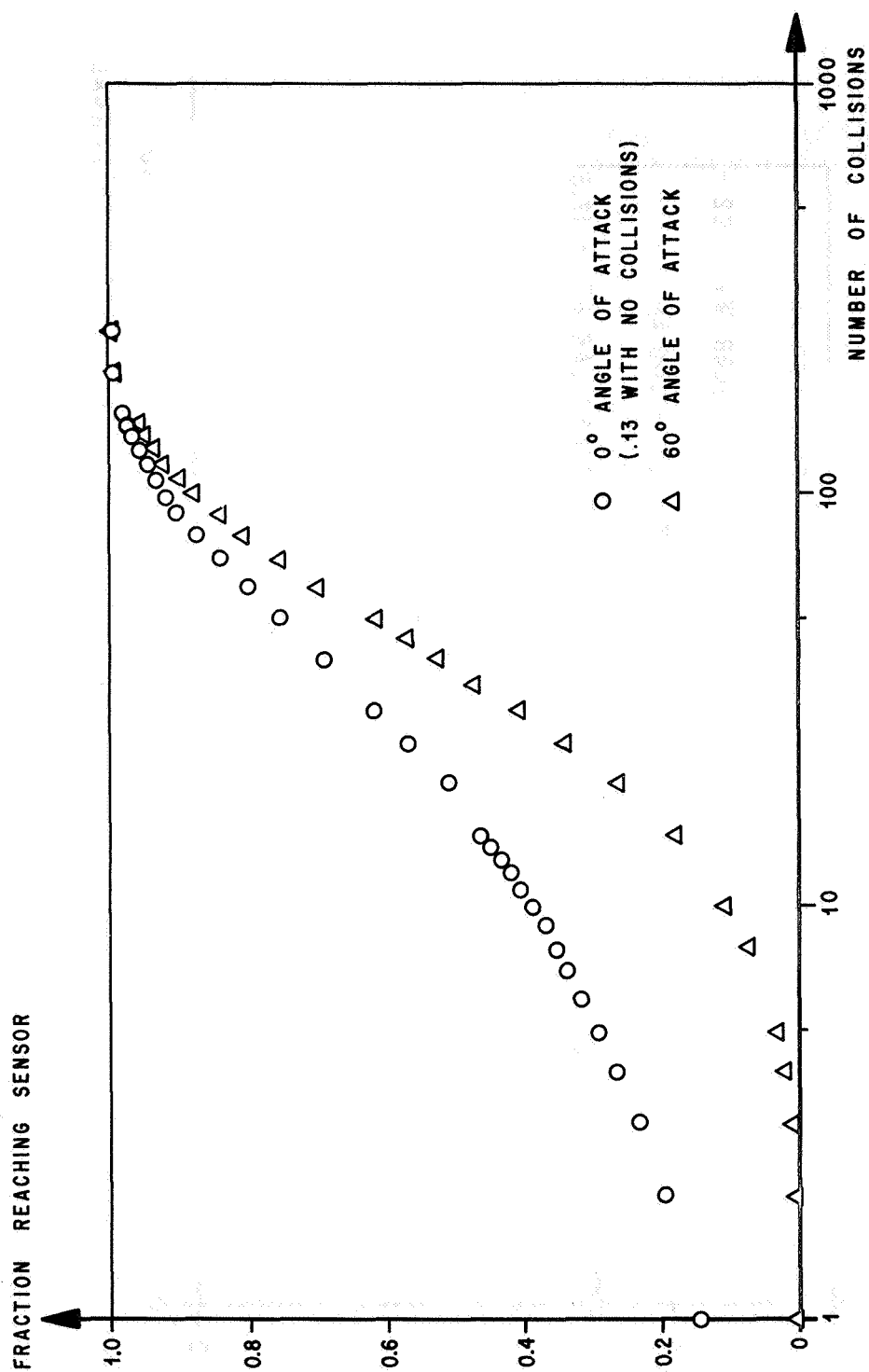


Figure 24. Fraction of Molecules Reaching Sensor as a Function of Wall Collisions, Speed Ratio = 8, Diffuse Reflections Redhead Gauge

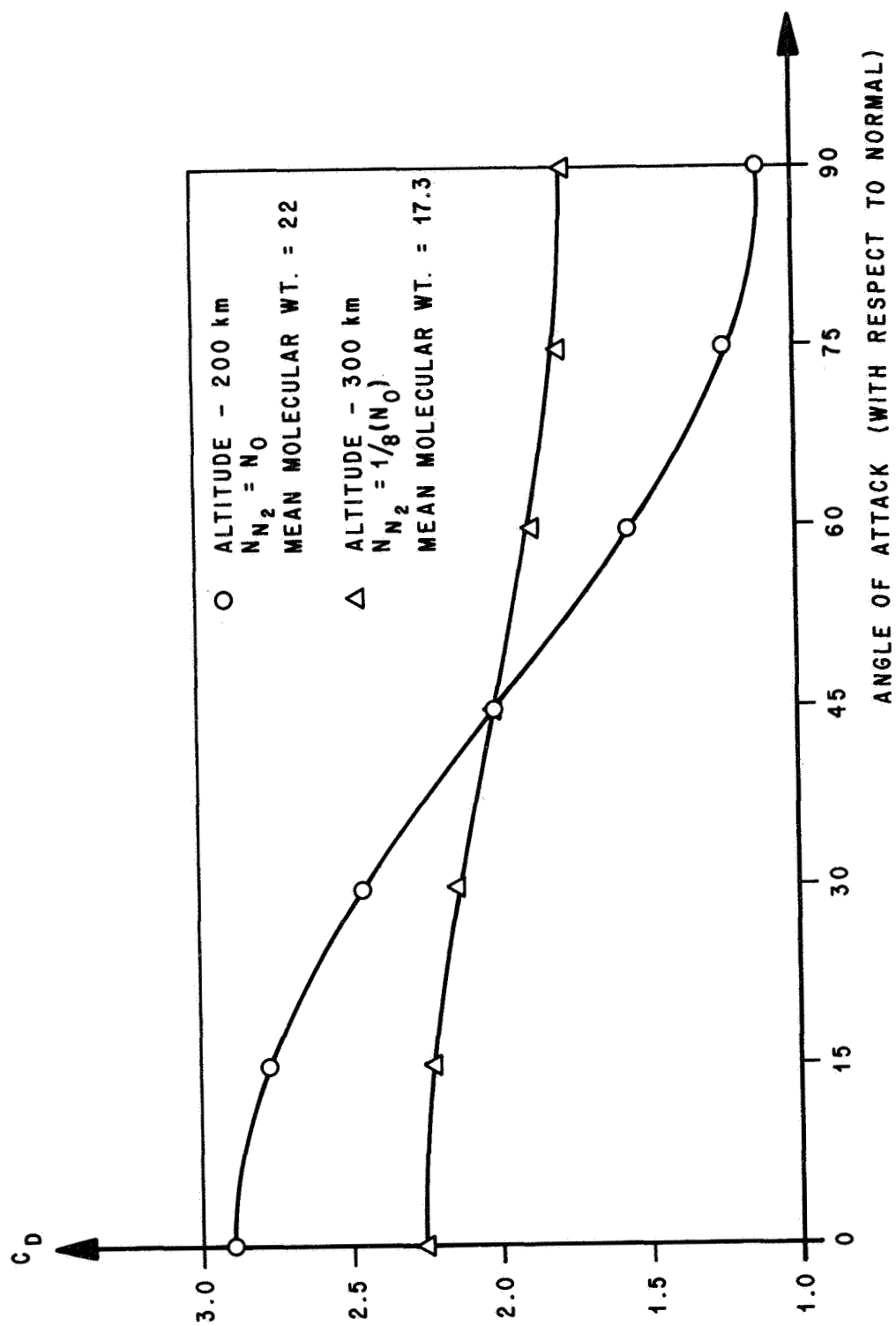


Figure 25. Theoretical Drag Coefficients for a Flat Plate  
 Specular Reflections for  $N_2$  - Accommodation Coefficient = 0.5  
 Diffuse Reflections for 0 - Accommodation Coefficient = 1.0



## REFERENCES

1. Newton, G. P., R. Horowitz, and W. Priester: "Atmospheric Densities from Explorer 17 Density Gauges and a Comparison with Satellite Drag Data," J. of Geophysical Res., Vol. 69, p. 4690, 1964.
2. Newton, G. P., D. T. Pelz, and W. Priester: "Atmospheric Density and Temperature Variations from Explorer XVII Satellite and a Further Comparison with Satellite Drag," Planetary and Space Sci., Vol. 13, pp. 599-616, 1965.
3. Cook, G. E.: "On the Accuracy of Measured Values of Upper Atmosphere Density," J. Geophysical Res., Vol. 70, No. 13, pp. 3247-3248, 1965.
4. Friedman, M. P.: "A Critical Survey of Upper-Thermosphere Density Measurements by Means of Ionization Gauges," Smithsonian Astrophysics Observatory Special Report 217, 1966.
5. Moe, Kenneth: "Absolute Atmospheric Densities Determined from the Spin and Orbital Decays of Explorer VI," COSPAR, International Space Symposium, 7th, Vienna, Austria, May 10-19, 1966.
6. Moe, Mildred M. and Kenneth Moe: "The Roles of Kinetic Theory and Gas-Surface Interactions in Measurement of Upper Atmosphere Density," Sixth Rarefied Gas Dynamics Symposium, Boston, Mass., July 1968.
7. Newton, G. P., D. T. Pelz, G. E. Millen, and R. Horowitz: "Response of Modified Redhead Magnetron and Bayard-Alpert Vacuum Gauges Aboard Explorer XVII," NASA X-651-63-243, 1963.
8. Newton, G., P. Silverman, and D. Pelz: "Interactions Between a Hypersonic Neutral Gas Beam and an Orificed Pressure Gauge Mounted in a Spinning Satellite," NASA X-621-68-396, 1968.
9. Newton, George P., David T. Pelz, and Hans Volland: "Direct in Situ Measurements of Wave Propagation in the Neutral Thermosphere," J. of Geophysical Res., Vol. 74, No. 1, pp. 267-271, 1969.
10. Pelz, D. and G. Newton: "Pressure Conversion Constant for Magnetron Ionization Gauges," J. Vac. Sci. Tech., Vol. 4, p. 239, Sept.-Oct. 1967.
11. Pelz, David T. and George R. Newton: "Midlatitude Neutral Thermosphere Density and Temperature Measurements," J. of Geophysical Res., Vol. 74, No. 1, January 1969.

#### REFERENCES (Continued)

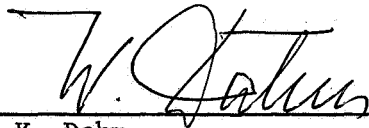
12. Ballance, James O.: "The Molecular Kinetics of the Bayard-Alpert and Modified Redhead Vacuum Gauges used on Explorer XVII and XXXII," NASA TM X-53838, 1969.
13. Ballance, James O.: "An Analysis of the Molecular Kinetics of the Thermosphere Probe," NASA TM X-53641, 1967.
14. Hedin, A. E., C. P. Avery, and C. D. Tschetten: "An Analysis of Spin Modulation Effects on Data Obtained with a Rocket-Borne Mass Spectrometer," J. Geo. Res., Vol. 69, No. 21, pp. 4637-4648, 1964.
15. Von Zahn, U.: "Mass Spectrometric Measurements of Atomic Oxygen in the Upper Atmosphere: A Critical Review," J. Geo. Res., Vol. 72, No. 23, pp. 5933-5937, 1967.
16. Zhukov, A. P., N. A. Sokova, and A. F. Chizhov: "Instruments for Measuring Temperatures and Partial Density of Molecular Nitrogen in the Upper Atmosphere," Trudy Tsentralnoy Aerologidieskoy Observatorii, No. 77, Gidrometeoizdat, Moscow, 1967, pp. 51-53.

A NEW INTERPRETATION OF THE EXPLORER XVII  
AND EXPLORER XXXII IONIZATION GAUGE DATA AND  
ITS IMPLICATIONS TO ORBITAL ANALYSIS

by James O. Ballance

The information in this report has been reviewed for security classification. Review of any information concerning Department of Defense or Atomic Energy Commission programs has been made by the MSFC Security Classification Officer. This report, in its entirety, has been determined to be unclassified.

This document has also been reviewed and approved for technical accuracy.



W. K. Dahm  
Chief, Aerophysics Division



E. D. Geissler  
Director, Aero-Astrodynamics Laboratory

## DISTRIBUTION

DIR  
S&E-DIR  
A&TS-MS-IL (8)  
A&TS-MS-IP  
A&TS-MS-H  
DEP-T  
A&TS-PAT  
A&TS-TU (6)

S&E-ASTR  
Mr. Moore

S&E-SSL  
Mr. Heller  
Mr. Hembree

S&E-AERO  
Dr. Geissler  
Mr. Vaughan  
Mr. R. E. Smith  
Dr. Heybey  
Mr. J. Johnson  
Mr. J. Carter  
Mr. Baker  
Mr. Dahm  
Mr. Ballance (40)  
Mr. Horn  
Mr. Lindberg  
Dr. Lovingood  
Dr. DeVries  
Mr. D. Weidner  
Mr. G. Swenson

### EXTERNAL

Tech. & Sci. Info. Facility (25)  
Box 33  
College Park, Md.  
NASA Rep. (S-AK/RKT)

Langley Res. Center  
Langley Sta.  
Hampton, Va.

Lewis Res. Center  
21000 Brookpark  
Cleveland, Ohio  
Attn: Mr. L. Krause  
Mr. E. Richley  
Library

Goddard Space Flight Center  
Greenbelt, Md.  
Attn: Mr. G. Newton (10)  
Mr. N. W. Spencer (5)  
Dr. H. Niemann  
Library

JPL  
4800 Oak Grove Dr.  
Pasadena, Calif.

Ames Res. Center  
Moffett Field, Calif.

Manned Spacecraft Center  
Houston, Texas  
Attn: Library

Arthur D. Little, Inc.  
Cambridge, Mass.

Northrop Space Labs.  
Huntsville, Ala.

Aerospace Corp.  
El Segundo, Calif.  
Attn: Virginia Carter  
Barbara Ching  
D. D. Elliott  
Library

Smithsonian Institute  
Astrophysical Observatory  
Cambridge, Mass.

AEDC  
Arnold Air Force Station, Tenn.

EXTERNAL DISTRIBUTION (Continued)

ARO, Inc.  
AEDC  
Arnold Air Force Sta., Tenn.  
Attn: Library

Univ. of Ill.  
Urbana, Ill.  
Attn: Library  
Dr. Yen  
Dr. G. Karr

Mass. Inst. of Tech.  
Cambridge, Mass.  
Attn: Dr. R. Stickney  
Dr. L. Trilling  
Library

Univ. of Ala.  
University, Ala.  
Attn: Dr. W. Schaetzle  
Library

Ga. Inst. of Tech.  
Atlanta, Ga.  
Attn: Dr. A. B. Huang  
Library

Inst. of Aerophysics  
Univ. of Toronto  
Toronto, Canada  
Attn: P. C. Hughes  
Dr. G. N. Patterson  
Library

Cornell Aeronautical Lab., Inc.  
Buffalo, New York

McDonnell Douglas  
P. O. Box 516  
Attn: E. S. J. Wange  
St. Louis, Missouri

University of Minnesota  
Minneapolis, Minnesota  
Attn: Library  
Dr. D. O. Nier

Atlantic Res. Corp.  
Missile Systems Div.  
3333 Harbor Blvd.  
Costa Mesa, Calif. 92626  
Attn: Library  
Dr. R. Chuan  
Mr. D. Wallace

Univ. of Calif.  
Radiation Laboratory  
Livermore, Calif.  
Attn: Library  
Dr. Hurlbut

Lockheed Aircraft Corp.  
Huntsville, Ala.  
Attn: Dr. C. Fan  
Mr. J. Robertson  
Mr. H. Shirley  
Library

Brown Engineering Co.  
Huntsville, Ala.  
Attn: R. Watson  
Library

Heat Technology Lab.  
Huntsville, Ala.

Univ. of Mich.  
Ann Arbor, Michigan  
Attn: George Carignan  
Dr. Paul Hayes  
David Taeusch  
Library

NASA Hdqs.  
OSSA - R. Horowitz  
- Dr. Fellows  
- Mr. Dubin

OART - Mr. Schwartz

McDonnell Douglas Astronautics Co.  
Space Sciences Division  
Santa Monica, Calif.  
Attn: Dr. K. Moe